Journal of Holography Applications in Physics
Volume 2, Special Issue, Winter 2022, 1-77
© Available online at http://jhap.du.ac.ir
DOI: 10.22128/jhap.2022.001.0045

Journal of Holography Applications in Physics

Conference Proceedings

1st International Conference on Holography and its Applications (ICHA1 2022)

9-10, March 2022

Damghan, Iran

Committee of the ICHA1 2022
School of Physics, Damghan University (DU)
Tel: +98 - 23 - 35220236
Email: holography@du.ac.ir

Conference website: https://holography.du.ac.ir

Conference Proceedings of 1st International Conference on Holography and its Applications (ICHA1, 2022)

Edited by Dr. Behnam Pourhassan

Online ISSN: 2783-3518
Print ISSN: 2783-4778

DOI: 10.22128/jhap.2022.001.0045

Published by Journal of Holography Applications in Physics (JHAP), Damghan University Press.
Tel: +98-23-35220236
Fax: +98-23-35220236

Hosting:
Damghan University, Damghan, Iran

Organized By:
School of Physics, Damghan University, Damghan, Iran

Academic Partner:
Canadian Quantum Research Center (CQRC)

ICHA1 2022 Executive Committee

Dr. Leila Shahkarami (Chief Executive Officer) *School of Physics, Damghan University, Damghan, Iran*

Morteza Tavakoli (Responsible for DU conferences) *Damghan University, Damghan, Iran*

Yasin Alipour (IT Head) *Damghan University, Damghan, Iran*

Jafar Mohammadi (Executive Committee member) *Damghan University, Damghan, Iran*

Hassan Azimi (Executive Committee member) *School of Physics, Damghan University, Damghan, Iran*

Reza Kalami (Executive Committee member) *Semnan University, Semnan, Iran*

ICHA1 2022 Session Chairs

Dr. Behnam Pourhassan *School of Physics, Damghan University, Damghan, Iran*

Dr. Kazem Bitaghsir Fadafan *Shahrood University of Technology, Iran*

Dr. Leila Shahkarami *School of Physics, Damghan University, Damghan, Iran*

Prof. Emmanuel Saridakis *Institute for Astronomy, Astrophysics, Space Applications and Remote Sensing (IAASARS), National Observatory of Athens, Athens, Greece*

Prof. Pietro Colangelo *National Institute for Nuclear Physics, Italy*

Dr. Haidar Sheikhahmadi *North-West University, South Africa*

ICHA1 2022 Scientific Committee

Dr. Behnam Pourhassan	(Conference Chair)	*School of Physics, Damghan University, Iran*
Prof. Salvatore Capozziello		*Napoli University, Italy*
Prof. Robert Mann		*University of Waterloo, Canada*
Prof. Saifollah Rasouli		*Institute for Advanced Studies in Basic Sciences, Iran*
Prof. Pietro Colangelo		*National Institute for Nuclear Physics, Italy*
Prof. Emre Onur Kahya		*Istanbul Technical University, Turkey*
Prof. Ligang Wang		*Zhejiang University, China*
Prof. Mir Faizal		*Canadian Quantum Research Center, Canada*
Dr. Kazem Bitaghsir Fadafan		*Shahrood University of Technology, Iran*
Dr. Hesam Soltanpanahi		*Jagiellonian University, Poland*
Dr. Reza Fareghbal		*Shahid Beheshti Universi, Iran*
Dr. Seyed Hossein Hendi		*Shiraz University, Iran*
Dr. Barun Majumder		*University of Tennessee, USA*
Dr. Ehsan Ahadi Akhlaghi		*Institute for Advanced Studies in Basic Sciences, Iran*
Dr. Saheb Soroushfar		*Yasouj University, Iran*
Dr. Haidar Sheikhahmadi		*North-West University, South Africa*
Dr. Azam Kardan		*School of Physics, Damghan University, Iran*
Dr. Leila Shahkarami		*School of Physics, Damghan University, Iran*

ICHA1 2022 Editorial Board

Message From the Conference Chair ICHA1 2022

Hello and welcome to the first International Conference on Holography and its Applications (ICHA). The school of physics at Damghan University recently tried to understand more about Holography. So, we established an international journal about Holography and related topics (JHAP). In the first volume, we published brilliant papers using the ribbon cut by Susskind.

We dedicated the second volume to the memory of Prof. John D. Barrow, the famous scientist who has introduced a deformed black hole entropy that is used to construct a holographic model of dark energy. Our first talk in this conference is about that.

Some of the authors in the first and second volumes of JHAP will talk about their papers at this conference and some of them talk about their new works.

This conference is a joint activity between the school of physics at Damghan university and the Canadian Quantum Research Center.

This conference included three parts of presentations:

In the first part, we had 5 talks by keynote speakers.

In the second part, we had some invited speakers which talked about their recent studies, some of them published by high-level journals.

In the third part, we had the selected talks or poster presentations among some of the abstracts and full papers submitted to ICHA 2022.

Dr. B. Pourhassan,

Conference Chair ICHA1 2022,
School of Physics,
Damghan University,
Iran

Message From the Chief Editor ICHA1 2022

Damghan University

Ladies and Gentleman

On behalf of Journal of Holography Applications in Physics (JHAP) and also School of Physics at Damghan University, allow me to extend a warm welcome to all of you. Welcome to 1th International Conference on Holography and its Applications in Physics. I would like to take this opportunity to talk you briefly about recent progress in Holography and our publications at School of Physics.

As we know, Holographic phenomena are consolidating their position in the scientific community. Today, quantum Holography and classical one cover all area of physics, from modern optics and nano photonics, theoretical physics to theoretical and experimental condensed matter physics. The phenomena related to Holography are showing their applications more and more in human society.

Classical holography techniques have been very successful in areas ranging from microscopy and fundamental research to manufacturing. However, imaging objects with light outside the visible range of the electromagnetic spectrum is a challenge. Researchers have invented a new quantum holography technique that images objects using undetected light. This counterintuitive process, which involves two correlated beams of nonclassical light in an interferometer, could find applications in biomedical imaging and other areas where the wavelengths of light best suited for imaging are technically challenging to detect.

Due to the increasing progress and success of holography, researchers at the School of Physics at Damghan University decided to publish an international journal to reflect the views and latest findings of scientists interested in holography. As expected, the publication of this journal soon attracted the attention of interested people.

Journal of Holography Applications in Physics (JHAP) covers all areas related to the holographic principle in physics. Holographic principle prepares the powerful tools to study several phenomena in various branches of physics. The aim of JHAP is to collect all applications of holography for the theoretical and experimental communities. We would like to publish high-quality peer-reviewed papers, free of charge and open access for all authors and readers. JHAP is fully sponsored by Damghan University. The reviewing and publishing process is completely free of charge.

This conference is held to celebrate the opening of JHAP. Our aim is to bring together holographic scientists in a specialized collection. We would to make a large group of who works holography. I hope that the topics and papers discussed at the conference will pave the way for holographic development. In addition, I invite all researchers to submit their latest findings on holography for publication in JHAP. I wish all the participants in the conference happy moments.

Prof. S A Ketabi,

Editor-in-Chief, JHAP

Damghan University,
Iran

Message From the Academic Partner Administrative ICHA1 2022

Please see the following links.

Mir Faizal Message Link: https://holography.du.ac.ir/en/files.php?rid=12

Scott Jacobsen Message Link: https://holography.du.ac.ir/en/files.php?rid=13

Table of Contents

Part One

Keynote Speakers

Symmetries at Causal Boundaries

Shahin Sheikh-Jabbari

School of Physics, Institute for Research in Fundamental Sciences (IPM), Tehran, Iran

Abstract: We consider gravity in 2 and 3 dimensions on a spacetime with a causal (timeline or null) codimension 1 boundary. We construct the solution space in these cases and study boundary symmetries and charges using covariant phase space formalism. We study surface charges which are functions at the causal boundary and label boundary degrees of freedom. We discuss algebra of charge which in general depends on the slicing of solution phase space. For the 3-dimensional case we show this algebra, in an appropriate slicing, is a direct sum of Heisenberg algebra and two copies of Virasoro (for AdS3 gravity) or BMS3 (for flat 3d gravity).

Talk link: https://www.aparat.com/v/w5TXf

Wednesday 9th March 2022

Entanglement in the quantum Hall matrix model

Sean A Hartnol

Cambridge University, Cambridge, UK

Abstract: Quantum mechanical theories describing large N by N matrices of oscillators can lead to an emergent space as N -> infinity. In the most fully fledged version, the emergent space is dynamical and gravitating. However, there are also simpler, lower dimensional versions of this phenomenon. One of the simplest occurs in the so-called quantum Hall matrix model, in which a 2-dimensional space emerges and supports Chern-Simons dynamics. I will describe how this solvable model leads to insights about the emergence of space from matrices. In particular, I will describe how the emergent spatial locality is reflected in the entanglement structure of the ground state of theory.

Talk link: https://aparat.com/v/wQyOG

Wednesday 9th March 2022

A Hilbert Space for Chern Simons Matter Theories

Shiraz Minwalla

Tata Institute of Fundamental Research, Mumbai, India

Abstract: See talk video.

Talk link: https://www.aparat.com/v/gIHhF

Thursday 10th March 2022

Conformal Surface Defects in Maxwell Theory are Trivial

Christopher P. Herzog

King's College, London, UK

Abstract: I consider a free Maxwell field in four dimensions in the presence of a codimension two defect. Reflection positive, codimension two defects which preserve conformal symmetry in this context are very limited. Only generalized free fields can exist on the defect and interact with the free Maxwell field in the bulk. This result stands in stark contrast to the codimension one case where interacting conformal boundary conditions can be found for free bulk fields, producing systems with physical relevance, for example for graphene.

Talk link: https://aparat.com/v/jYOIZ

Thursday 10th March 2022

Puzzles and Questions about Entropy and Information Loss (and AdS/CFT)

Bernard S Kay

University of York, UK

Abstract: We recall the puzzles about quantum black holes, including the information loss puzzle, the thermal atmosphere puzzle and the firewall puzzle, and we emphasize the importance of identifying what corresponds to 'physical entropy' in any theoretical framework that attempts to resolve them. The currently favoured approach identifies it with "coarse grained entropy" and this is a bit surprising given its notoriously subjective character and given that, soon after Hawking announced his 1974 black hole evaporation result, there were hopes that a new understanding of entropy would emerge that had a more objective character. We also point out some other difficulties with the assumptions (some explicit, some implicit) underlying the current approach and argue that some of these difficulties -- and indeed the puzzles themselves -- might be resolved if one were, instead, to adopt my 1998 matter gravity entanglement hypothesis in which physical entropy is identified with matter-gravity entanglement entropy. We also argue that this alternative approach to resolving the puzzles suggests that the AdS-CFT correspondence is not a bijection from the boundary CFT to full quantum gravity in the bulk but rather just to the bulk "matter sector". This raises the question of what the matter-gravity split consists of in quantum gravity/string theory.

Talk link: https://aparat.com/v/2vPbI

Thursday 10th March 2022

Part Two

Invited Talks

Inflation driven by Barrow Holographic dark energy

Prabir Rudra

University of Calcutta, India

Abstract: In this work we have investigated the inflation mechanism driven by the Barrow Holographic dark energy (BHDE) in the early universe. BHDE is based on the Barrow relation for horizon entropy, which in turn is inspired from the shape of the COVID-19 virus. It was shown by Barrow that the quantum gravitational effects may instigate complex fractal features in the structure of a black hole. Since the length scale during the inflation is expected to be small, the energy density obtained from the application of the holographic principle in the early universe will be large enough to support the inflationary scenario. Using the Granda-Oliveros IR cut-off we have studied the inflationary scenario with the universe filled with BHDE. Various analytic solutions for the model were found out including the slow-roll parameters, scalar spectral index and tensor-to-scalar ratio. Since inflation is generally attributed to the presence of scalar fields, we have explored a correspondence between BHDE and scalar field models. Both canonical scalar field and the Tachyonic scalar field have been considered for this purpose. The evolution of the potential generated from the fields are plotted and found to be consistent with the observations. From the work we see that BHDE can be a model of dark energy that can successfully drive the early time inflation.

Talk link: https://www.aparat.com/v/evon5

Wednesday 9th March 2022

Holographic Dark Energy, Triumphs and Drawbacks

Haidar Sheikhahmadi

Center for Space Research, North-West University, Mahikeng, South Africa,

School of Astronomy, Institute for Research in Fundamental Sciences (IPM), Tehran, Iran,

Canadian Quantum Research Center, British Columbia, Canada

Abstract: In this article, we will try to examine the successes and problems of a model of dark energy called the holographic model. This model, which has its roots in gravitational quantum and topics related to the entropy of black holes, in recent years has found very significant applications in cosmological topics related to the early universe or the late universe. Despite these very valuable successes, but also suffers from some problems. For example, issues related to causality that the standard holographic model cannot describe correctly. But I have shown in this work that the problem goes even further. The main paper proposing the application to cosmological topics seems to have erred in defining the relationship between the ultraviolet and infrared cutoffs so that energy density can no longer be defined in such a way that the inverse quadratic power can be considered. On the other hand, when considering the experiment related to electron gyromagnetic anomalies, the results will show a significant difference from the proposed models and show a significant closeness to the proposed quantum gravity values.

Talk link: https://aparat.com/v/ImNEo

Wednesday 9th March 2022

Testing time evolution of the mass distribution of the black hole mergers

Teruaki Suyama

Tokyo Institute of Technology, Japan

Abstract: Detection of the gravitational-wave events revealed that there are numerous populations of the black hole binaries which can merge within the age of the Universe. Although several formation channels of such binaries are known, considerable theoretical uncertainties associated in each channel defeats the robust prediction of how much each channel contributes to the total merger rate density. Given that the time evolution of the merger rate density in some channels is independent of the BH masses, clarifying this feature from the observational data will shed some light on the nature of the black hole binaries. Based on this motivation, we formulate the methodology to perform the statistical test of whether the mass distribution of the black hole mergers evolves in time or not by means of the hypothesis testing. Our statistical test requires neither a priori specification of the mass distribution which is largely uncertain nor that of the time dependence of the merger rate. We then apply it to the mock data for some concrete shapes of the merger rate density and show that the proposed method rejects/(does not reject) the null hypothesis correctly for the large sample size. We also investigate if the catalog of the gravitational-wave events obtained during the LIGO-Virgo's third observing run has a large sample size enough to apply our hypothesis testing. We find that the number of the events is too small to draw any statistical conclusion regarding our test and the meaningful result of our hypothesis testing can be obtained only by the future detectors having much better sensitivity. These results demonstrate the effectiveness of our hypothesis testing to determine from the future observational data whether the merger rate density evolves in time independently of the BH masses or not.

Talk link: https://aparat.com/v/X5sGy

Wednesday 9th March 2022

Simple Bulk Reconstruction in AdS/CFT Correspondence

Seiji Terashima

YITP, Kyoto, Japan

Abstract: We show that the bulk reconstruction in the AdS/CFT correspondence is rather simple and has an intuitive picture, by showing that the HKLL bulk reconstruction formula can be simplified. We also reconstruct the wave packets in the bulk theory from the CFT primary operators. With these wave packets, we discuss the causality and duality constraints and find our picture is only the consistent one. Our picture of the bulk reconstruction can be applied to the asymptotic AdS spacetime.

Talk link: https://www.aparat.com/v/l24QX

Wednesday 9th March 2022

A two-sheeted, CPT-symmetric universe

Latham Boyle

Perimeter Institute for Theoretical Physics, Canada

Abstract: Our universe seems to be radiation dominated at early times, and vacuum energy dominated at late times. When we consider the maximal analytic extension of this spacetime, its symmetries and complex analytic properties suggest a picture in which spacetime has two sheets, exchanged by an isometry which, in turn, picks a preferred (CPT-symmetric) vacuum state for quantum fields on the spacetime. I will explain how this line of thought makes several testable predictions and suggests new explanations for dark matter, the arrow of time, and various observed properties of the primordial perturbations. I will also introduce a related intriguing point: how a certain set of dimension-zero scalar fields, which automatically have a scale-invariant spectrum of vacuum fluctuations, also seem to "fix" the standard model vacuum, through a non-trivial cancellation of the vacuum energy and both terms in the Weyl anomaly.

Talk link: https://www.aparat.com/v/LmeB5

Wednesday 9th March 2022

Gravitational entropy and the large scale geometry of spacetime

Neil Turok

Higgs Centre for Theoretical Physics, James Clerk Maxwell Building, UK
Perimeter Institute, Ontario, Canada

Abstract: I'll review a new, simpler explanation for the large scale geometry of spacetime, presented in our recent preprint arXiv:2201.07279. The basic ingredients are elementary and well-known, namely Einstein's theory of gravity and Hawking's method of computing gravitational entropy. The new twist is provided by the boundary conditions we proposed for big bang-type singularities, allowing conformal zeros but imposing CPT symmetry and analyticity at the bang. These boundary conditions allow gravitational instantons for universes with positive Lambda, massless radiation and positive or negative space curvature. We are thus able to infer the gravitational entropy for a complete set of semi-realistic, four-dimensional cosmologies. We find that the gravitational entropy can be significantly larger than the de Sitter entropy. To the extent that it is, the most probable large-scale geometry for the universe is flat, homogeneous and isotropic. I will briefly summarize what remains to be done to develop this picture into a principled and fully predictive theory of the cosmos.

Talk link: https://www.aparat.com/v/N4p1G

Wednesday 9th March 2022

Quantum Gravitational Corrections to the Entropy of a Reissner-Nordström Black Hole

Ruben Campos Delgado

Bethe Center for Theoretical Physics
and
Physikalisches Institut der Universitat Bonn, Germany

Abstract: Starting from an effective action for quantum gravity, we calculate the quantum gravitational corrections to the Wald entropy of a four-dimensional non-extremal Reissner-Nordström (RN) black hole in the limit of small electric charge, generalising a previous calculation carried out by Calmet and Kuipers for a Schwarzschild black hole. We show that, at second order in the Ricci curvature, the RN metric receives quantum corrections which shift the classical position of the event horizon. We apply the Wald entropy formula by integrating over the perimeter of the quantum corrected event horizon. We then compute the quantum gravitational corrections to the temperature and the pressure of the black hole.

Talk link: https://www.aparat.com/v/jaK84

Wednesday 9th March 2022

Holographic boundary actions in AdS3/CFT2 revisited

Kevin Nguyen

Department of Mathematics, King's College London, London, United Kingdom

Abstract: Various kinds of boundary actions have appeared over the years in the context of pure AdS3 gravity. One of them is the generating functional of stress tensor correlation functions of a dual holographic CFT. Others, obtained by Hamiltonian reduction of pure gravity in its Chern-Simons formulation, describe the dynamics of the only dynamical degrees of freedom residing at the conformal boundary. I will review these various actions and emphasize their differences. I will further discuss the role they play in the recent proposal that pure AdS3 gravity is dual to a random matrix ensemble.

Talk link: https://aparat.com/v/W321d

Wednesday 9th March 2022

Holographic RG Flows for Kondo-like Impurities

Christian Northe

Institut fur Theoretische Physik und Astrophysik Würzburg, Germany

Abstract: Boundary, defect, and interface RG flows, as exemplified by the famous Kondo model, play a significant role in the theory of quantum fields. We study in detail the holographic dual of a non-conformal supersymmetric impurity in the D1/D5 CFT. Its RG flow bears similarities to the Kondo model, although unlike the Kondo model the CFT is strongly coupled in the holographic regime. The interface we study preserves $d = 1$, N=4 supersymmetry and flows to conformal fixed points in both the UV and IR. The interface's UV fixed point is described by $d = 1$ fermionic degrees of freedom, coupled to a gauge connection on the CFT target space that is induced by the ADHM construction. We briefly discuss its field-theoretic properties before shifting our focus to its holographic dual. We analyze the supergravity dual of this interface RG flow, first in the probe limit and then including gravitational backreaction. In the probe limit, the flow is realized by the puffing up of probe branes on an internal S^3 via the Myers effect. We further identify the backreacted supergravity configurations dual to the interface fixed points. These supergravity solutions provide a geometric realization of critical screening of the defect degrees of freedom. This critical screening arises in a way similar to the original Kondo model. We compute the g-factor both in the probe brane approximation and using backreacted supergravity solutions, and show that it decreases from the UV to the IR as required by the g-theorem.

Talk link: https://holography.du.ac.ir/en/files.php?rid=27

Wednesday 9th March 2022

A Weyl Semimetal from AdS/CFT with Flavour

Ronald Rodgers[1], Kazem Bitaghsir Fadafan[2], Andy O'Bannon[3], Matthew Russell[3]

1-Nordita Sweden,

2-Shahrood University,

3-Southampton University

Abstract: Weyl semimetals (WSMs) are a class of materials with electronic bands that have topologically-protected point-like intersections in momentum space, at an energy near the Fermi level. The low energy excitations of a WSM are Weyl fermions, and the resulting chiral anomaly leads to interesting transport behaviour. Due to weak screening, the Coulomb interaction in WSMs can become strong, and holography may be useful to understand the resulting physics. I will describe a top-down holographic model of a WSM, in which a D7-brane in AdS5 x S5 is coiled into a helix. The holographic dual is N=4 super-Yang-Mills theory coupled to N=2 hypermultiplets, with an external axial gauge field. I will compute the electrical conductivities of this system, as a probe of the anomalous transport.

Talk link: https://www.aparat.com/v/yTWXn

Wednesday 9th March 2022

Magnetically-induced Holographic Composite Inflation

Amjad Ashoorioon

School of Physics, Institute for Research in Fundamental Sciences (IPM), Tehran, Iran

Abstract: We study the observational predictions of the phenomenological anti-de Sitter (AdS)/QCD inspired model, in which the inflaton field emerges in a four-dimensional strongly coupled gauge theory, in which the chiral symmetry breaking occurs through the formation of the quark condensate. Based on a top-down approach of AdS/QCD, using a D7-brane in the background of N_c D3-branes, it has already been shown that chiral symmetry breaking in a magnetic field through the generation of the Higgs vacuum expectation value could be a second-order phase transition, although it was doubted that this scenario could lead to enough inflation. Using an iterative method, we consistently solve for the time-dependent parameters, including the embedding function of the D7-brane and the Hubble parameter of the expanding background. We show that with $N_c \sim 10^7$ and $g_{UV} \sim$ few 0.1, the predictions of the inflationary model are consistent with the most stringent constraints placed on the inflationary models by Planck 2018. Although the model is capable of producing a large amount of gravitational waves, $\simeq 0.01$, the displacement of the canonical mass dimension-1 scalar field remains below the Planck mass, in violation of the Lyth bound.

Talk link: https://aparat.com/v/Uwc5W

Wednesday 9th March 2022

A perturbative CFT dual for pure NS-NS AdS3 strings

Lorenz Eberhardt

School of Natural Sciences, Institute for Advanced Study, Princeton, USA

Abstract: A proposal is made for a CFT dual to string theory on AdS3 with pure NS-NS flux. It is given by a symmetric orbifold of a linear dilaton theory deformed by a marginal operator from the twist-2 sector. I explain the matching of the full spectra of short and long strings and the matching of correlation functions at genus 0. The duality should be understood as perturbative in 1/N.

Talk link: https://aparat.com/v/GAr2E

Wednesday 9th March 2022

Flat-space limit of AdS/CFT

Yue-Zhou Li

Department of Physics, McGill University, Canada

Abstract: There are different descriptions of extracting amplitudes from taking the flat-space limit of AdS/CFT, include momentum space, Mellin space, coordinate space, partial-wave expansion, and impact parameter space. We will review the first three descriptions. We will then show how to connect them and explain the common origin. Finally, we will discuss a possible generalization to spinning operators.

Talk link: https://aparat.com/v/xgNFR

Wednesday 9th March 2022

Thermodynamic Phase Transition of Generalized Ayon-Beato Garcia Black Holes with Schwarzschild anti de Sitter space time perspective

Hossein Ghaffarnejad, Elham Ghasemi

Semnan University, Semnan, Iran

Abstract: In this work we study thermodynamics of generalized Ayon-Beato and Garcia (ABG) black hole metric which contains three parameters named as mass m, magnetic charge q and dimensionless coupling constant of nonlinear electrodynamics interacting field γ. This is done at extended phase space where we need a cosmological parameter which behaves as the pressure thermodynamic coordinate. We generate the necessary cosmological parameter from the charge parameter of the ABG metric field. In short, we first extract a variable cosmological parameter together with a variable mass function such that the ABG black hole metric can be shown similar to a Schwarzschild anti de Sitter form apparently. Then by calculating the Hawking temperature of the black hole we obtain equation of state. By studying isothermal P-V curves we infer that the system participates in the Hawking-Page phase transition where the disequilibrium evaporating ABG black hole reaches finally to a vacuum AdS space. Other diagrams such that Gibbs free energy, heat capacity and entropy satisfy possibility of phase transition and there is also a coexistence point in phase space depended to γ value where the two different phases exist synchronously. For small scale black holes there are three phases while for larger than there are just two phases.

Talk link: https://www.aparat.com/v/vGdeZ

Wednesday 9th March 2022

Rotating counterpart of Lee-Wick black hole and its thermodynamics

Sudhaker Upadhyay

Department of Physics, K. L. S. College, Nawada, India

Abstract: We study a singular solution for the rotating counterpart of Lee-Wick gravity having a point source in a higher-derivative theory. We critically analyze the thermodynamics of such thermal system by evaluating mass parameter, angular velocity and Hawking temperature. The system follows first-law of thermodynamics and leads to the expression of entropy. We further discuss the stability and phase transition of the theory by evaluating heat capacity and free energy. The phase transition occurs at the point of divergence and the temperature is maximum. Remarkably, the black hole is unstable for small horizon radius and stable for large horizon radius.

Talk link: https://holography.du.ac.ir/en/files.php?rid=16

Thursday 10th March 2022

Evolutions in first-order viscous hydrodynamics

Yago Bea

Department of Physics and Helsinki Institute of Physics, University of Helsinki, Finland

Abstract: Motivated by the physics of the quark-gluon plasma created in heavy-ion collision experiments, we use holography to study the regime of applicability of various theories of relativistic viscous hydrodynamics. Using the microscopic description provided by holography of a system that relaxes to equilibrium, we obtain initial data with which we perform real-time evolutions in 2+1 dimensional conformal fluids using the first-order viscous relativistic hydrodynamics theory of Bemfica, Disconzi, Noronha and Kovtun (BDNK), BRSSS and ideal hydrodynamics. By initializing the hydrodynamics codes at different times, we can check the constitutive relations and assess the predictive power and accuracy of each of these theories.

Talk link: https://aparat.com/v/gFbQR

Thursday 10th March 2022

Scalarized black holes in Horndeski gravity: an overview

Ludovic Ducobu

University of Mons, Belgium

Abstract: General Relativity [GR] offers an extremely successful framework to describe the gravitational interaction whose achievements range from the solar system to the cosmological scale. Nonetheless, despite those undeniable success, the necessity to question the framework of GR is clear at both the experimental and theoretical level. On the one hand, the lack of explanation for the origin and composition of dark matter and dark energy reveals the necessity to extent GR on an experimental basis. On the other hand, the interpretation of spacetime singularities and the elusiveness of a consistent UV completion of the theory motivates a "reworking" of GR from a purely theoretical point of view. Since not all of the aforementioned puzzles can be purely reduced to quantum correction problems, this motivates the study of alternative theories of gravitation already at the classical level. Among the many possible directions one can follow, a very interesting one consist in the addition of new degrees of freedom in the theory (in addition to the spacetime metric) and, in this respect, the simplest candidate is a scalar field. We then obtain the framework of a scalar-tensor theory of gravity. In this talk, I will review the main features of Horndeski gravity and comment on black hole (BH) solutions known in this generic class of scalar-tensor theories of gravity. This journey will give us the opportunity to glimpse at the famous no-hair arguments limiting the possibility to endow BH with non-trivial scalar fields, to comment on the construction of Horndeski gravity and to review several interesting BH solutions known in scalar-tensor theories with coupling to the Gauss-Bonnet invariant or with derivative coupling to the Einstein-tensor. This talk, although self-contained, will be part of a three-part work with Sebastian Bahamonde and Christian Pfeifer aiming to present recent results obtained for scalarized black holes in scalar-torsion gravity, an alternative way to couple scalar fields to gravity.

Talk link: https://aparat.com/v/xanuJ

Thursday 10th March 2022

Scalarized Black Holes in Teleparallel Gravity

Sebastian Bahamonde

Department of Physics, Tokyo Institute of Technology, Tokyo, Japan

Abstract: An important question regarding black holes properties is to know if they can support "hairs". While this is famously forbidden in general relativity, in particular for scalar fields, by the so-called no-hair theorems, hairy black holes have been shown to exist in several classes of scalar-tensor theories of gravity. In this talk, I will show the existence of scalarized black holes in teleparallel scalar-torsion theories of gravity which is a formulation of gravity where the curvature is zero but the torsion tensor is non-vanishing. I will then present exact solutions for certain choices of couplings between a scalar field and the torsion tensor of a teleparallel connection and certain scalar field potentials, and thus proof the existence of scalarized black holes in these theories. On the other hand, I will also show that it is possible to establish no-scalar-hair theorems similar to what is known in general relativity for other choices of these functions.

Talk link: https://www.aparat.com/v/oMXT0

Thursday 10th March 2022

Entanglement Entropy and Phase Space Density: Lowest Landau Levels and 1/2 BPS states

Sinong Liu[1], Shaun Hampton[2], Sumit Das[3]

1-Faculty of Physics, University of Warsaw, Poland,

2-Institut de Physique Theorique, Universite Paris Saclay,

3-University of Kentucky

Abstract: We consider the entanglement entropy of an arbitrary subregion in a system of N non-relativistic fermions in $2+1$ dimensions in Lowest Landau Level (LLL) states. Using the connection of these states to those of an auxiliary $1+1$ dimensional fermionic system, we derive an expression for the leading large-N contribution in terms of the expectation value of the phase space density operator in $1+1$ dimensions. For appropriate subregions the latter can replaced by its semiclassical Thomas-Fermi value, yielding expressions in terms of explicit integrals which can be evaluated analytically. We show that the leading term in the entanglement entropy is a perimeter law with a shape independent coefficient. Furthermore, we obtain analytic expressions for additional contributions from sharp corners on the entangling curve. Both the perimeter and the corner pieces are in good agreement with existing calculations for special subregions. Our results are relevant to the integer quantum Hall effect problem, and to the half-BPS sector of $\mathcal{N}=4$ Yang Mills theory on S^3. In this latter context, the entanglement we consider is an entanglement in target space. We comment on possible implications to gauge-gravity duality.

Talk link: https://aparat.com/v/OQTa9

Thursday 10th March 2022

From Fields to Strings

Maity Pronobesh
International Centre for Theoretical Sciences-TIFR, India

Abstract: This talk is based on a paper available on arxiv with ID 2011.10038.

Talk link: https://holography.du.ac.ir/en/files.php?rid=25

Thursday 10th March 2022

Reflected entropy in Galilean conformal field theories

Vinayak Raj

Indian Institute of Technology Kanpur, India

Abstract: We obtain the reflected entropy for bipartite states in a class of $(1+1)$-dimensional Galilean conformal field theories ($GCFT_{1+1}$) through a replica technique. Furthermore, we compare our results with the entanglement wedge cross section (EWCS) obtained for the dual $(2+1)$-dimensional asymptotically flat geometries in the context of flat space holography. We find that our results are consistent with the duality between the reflected entropy and the bulk EWCS for flat holographic scenarios.

Talk link: https://holography.du.ac.ir/en/files.php?rid=23

Thursday 10th March 2022

Recent progress and challenges in (2,2) AdS_3/CFT_2

Arash Ardehali

Stony Brook University, Stony Brook, New York, USA

Abstract: I will discuss recent progress in joint work with Jiang and Zhao on going beyond the classical supergravity approximation in (2,2) AdS_3/CFT_2, and also highlight a few lingering puzzles.

Talk link: https://aparat.com/v/IdENW

Thursday 10th March 2022

Quantum Black Holes: from holography to scrambling and gravitational wave astronomy

Niayesh Afshordi

University of Waterloo, Canada

Abstract: I will talk about how recent advances in observations of gravitational waves can be used to probe the quantum nature of black hole horizons, and what it can teach us about quantum chaos and holography.

Talk link: https://aparat.com/v/cZUpz

Thursday 10th March 2022

Spin Impurities, Wilson Lines and Semiclassics

Gabriel Cuomo

Simons Center for Geometry and Physics, SUNY, Stony Brook, NY USA

Abstract: I will discuss line defects with large quantum numbers in conformal field theories. First, I will consider spin impurities, both for a free scalar triplet and in the Wilson-Fisher O(3) model. I will describe a new semiclassical approach, that allows charting the phase diagram; I will thus obtain numerous rigorous predictions for large spin impurities in 2+1 dimensional magnets. Using similar techniques, I will also derive a universal effective field theory (EFT) description for 1/2-BPS Wilson lines in large representations of the gauge group in rank-1 N=2 superconformal field theories. For Lagrangian theories, the EFT predictions are confirmed by exact localization results. Based on 2202.00040 with Zohar Komargodski, Márk Mezei, and Avia Raviv-Moshe.

Talk link: https://aparat.com/v/a3Skl

Thursday 10th March 2022

Part Three

Oral and poster presentations

Full paper - Oral

Modified cosmic Chaplygin gas and its holographic dual

Behnam Pourhassan
School of physics, Damghan University, Damghan, Iran.
Email: b.pourhassan@du.ac.ir

Abstract. In this paper, a charged black hole in the AdS space is introduced, which reflects the properties of the cosmic modified Chaplygin fluid. A similar model has already been constructed using modified Chaplygin fluid and an uncharged black hole. Therefore, in this paper, we are faced with two new parameters, which are the electric charge and the cosmic parameter, which we can study their effect on the thermodynamic stability of Chaplygin fluid and also on the resulting black hole. This paper is based on a preprint arxiv: 1910.00466 which is a joint work in collaboration with Ujjal Debnath.

Keywords: Black hole, Holography.

1 Introduction

Black holes are one of the most important topics in theoretical physics. This field of research enhances our knowledge of quantum gravity theory. One way to study black holes is to study their thermodynamics. By studying the thermodynamic behavior of black holes, it can be understood that some of them are the holographic dual of van der Waals fluid, that is, they behave thermodynamically like a van der Waals fluid [1, 2, 3].
These are known as van der Waals black holes, and the AdS black hole is one of them [4, 5, 6]. Negative cosmological constants in such black holes play the role of thermodynamic pressure [7]. This relationship between the black hole pressure and the cosmological constant raises the idea that a cosmological model with a given equation of state considers the holographic dual of a charged AdS black hole. Among the many models for dark energy in cosmology, in this paper we deal with the state equation of the cosmic modified Chaplygin gas and construct its dual black hole metric. In this way we can obtain important information about dark energy, which is one of the most important unknowns in physics today.

2 Equation of State

The equation of state, proposed by Chaplygin more than one hundred years ago in a study of the pressure on the wings of an airplane [8], has recently been considered as a model that describes dark energy. This equation of state is as follows:

$$p = -\frac{B}{\rho} \tag{1}$$

It is clear that a positive density leads to a negative pressure, and just as this negative pressure (upward) causes the plane to lift, it can also produce the accelerated expansion of the universe. But this model could not justify some observations, especially the conditions of the world today. Therefore, comparing the results obtained from this model with the observational data caused this state equation to be generalized as follows [9]

$$p = A\rho - \frac{\left(C+(\rho^{1+\alpha}-C)^{-w}\right)}{\rho^{\alpha}} \tag{2}$$

where

$$C = \frac{B}{1+w} - 1 \tag{3}$$

Cosmic parameter is a constant satisfied the following condition

$$-1 < w \leq 0 \tag{4}$$

The question now is, is there another thing in our universe that behaves like such a fluid? Various studies have shown that black holes can behave like fluids. The principles of holography allow us to study the behavior of black holes. Our goal now is to create a charged AdS black hole that behaves thermodynamically like a fluid with the equation of state (2).

3 Black Hole Metric

In spherical coordinates, space-time is described by four coordinates. A four-dimensional spherical symmetric black hole is generally described by the following metric

$$ds^2 = -f(r)dt^2 + \frac{dr^2}{f(r)} + r^2 d\Omega_2{}^2 \tag{5}$$

where

$$f(r) = \frac{r^2}{l^2} - \frac{2M}{r} + \frac{Q^2}{r^2} - g(r,\rho) \tag{6}$$

The curvature constant of the AdS space (which has a negative cosmological constant) is related to pressure as follows:

$$p = \frac{3}{8\pi l^2} \tag{7}$$

There is an unspecified function here that must be found so that the black hole we are looking at behaves like a cosmic modified Chaplygin fluid. One of our goals in this article is to find this function. The event horizon of this black hole given by the following relation

$$f(r) = 0 \tag{8}$$

which yields to r_h.

By combining relations (6), (7) and (8), we can express the mass of a black hole as follows

$$M = \frac{4\pi}{3} p r_h{}^3 + \frac{Q^2}{2r_h} - \frac{1}{2} r_h g(r_h,\rho) \tag{9}$$

Using this relation in the next section we can calculate the thermodynamic volume of the system. Using this equation, we can determine the temperature of the black hole and then calculate other thermodynamic quantities.

4 Thermodynamics

One of the best ways to study black holes is to study their thermodynamics. The entropy of our desired black hole is given in terms of the event horizon with the following relation

$$S = \pi r_h{}^2 \tag{10}$$

This relation is also valid for many other four-dimensional black holes, while temperature is related to the surface gravity of a black hole and is obtained from the following general formula

$$T = \frac{1}{4\pi}\left[\frac{\partial f(r)}{\partial r}\right]_{r=r_h} \tag{11}$$

The mass of the black hole plays the role of enthalpy hence of the thermodynamic relation

$$V = \left(\frac{\partial H}{\partial p}\right)_T = \left(\frac{\partial M}{\partial p}\right)_T \tag{12}$$

We can obtain the thermodynamic volume using Equation (9) as follows

$$V = \frac{4\pi}{3} {r_h}^3 - \frac{1}{2} r_h \frac{\partial g(r_h, \rho)}{\partial \rho} \left(\frac{dp}{d\rho}\right)^{-1} \tag{13}$$

After specifying the unknown function, we can obtain the thermodynamic volume. Also, the electric potential of the charged black hole is as follows

$$\Phi = \frac{\partial M}{\partial Q} = \frac{Q}{r_h} \tag{14}$$

In this case, using the first law of thermodynamics, we can obtain the following relation [10],

$$S = \frac{p+\rho}{T} V - \frac{\Phi Q}{T} \tag{15}$$

This is, in fact, the first law of thermodynamics for the charged AdS black hole, which is the Chaplygin fluid dual. Using this thermodynamic relationship, we can determine the unknown metric function and achieve our goals. Hawking [11, 12] and Bekenstein [13] showed that black holes behave like a thermodynamic system and that the laws of thermodynamics apply to them. Therefore, by studying the thermodynamics of a black hole, we can also obtain information about its dual fluid.

5 Solution

By using the relations (9) - (14) in Equation (15) we obtain the following relation

$$\frac{9{r_h}^2}{l^2} + \frac{9Q^2}{{r_h}^2} - 3g(r_h, \rho) - 3r_h \left[\frac{\partial g(r,\rho)}{\partial r}\right]_{r=r_h} - (\rho + p)\left[16\pi {r_h}^2 - 6\frac{\partial g(r_h, p)}{\partial p}\right] = 0 \tag{16}$$

Therefore, we use the method of separating variables and write

$$g(r,p) = X(r)Y(p) \tag{17}$$

By placing equation (17) in equation (16) we find the following solutions

$$X(r) = C_X e^{\frac{X_0 r}{3r_h}} \tag{18}$$

and

$$Y(p) = C_Y e^{\frac{8\pi l^2 (X_0+3){r_h}^4}{27(Q^2 l^2 + {r_h}^4)} p} \tag{19}$$

Hence

$$g(r,\rho) = C_{XY} e^G \tag{20}$$

where $C_{XY} = C_X C_Y$ and

$$G = \frac{X_0 r}{3r_h} + \frac{8\pi l^2 (X_0+3){r_h}^4}{27(Q^2 l^2 + {r_h}^4)} A\rho - \frac{8\pi l^2 (X_0+3){r_h}^4}{27(Q^2 l^2 + {r_h}^4)} \frac{\left(C + \left(\rho^{1+\alpha} - C\right)^{-w}\right)}{\rho^\alpha}$$

So, by putting equation (20) in (6) and using equation (3) we will have

$$f(r) = \frac{r^2}{l^2} - \frac{2M}{r} + \frac{Q^2}{r^2} - De^{\frac{r}{3}} \tag{21}$$

where $D = C_{XY} C_f$ and

$$C_f = e^{\frac{(X_0+3){r_h}^4}{9(Q^2 l^2 + {r_h}^4)} p} \tag{22}$$

Thus metric (5) with the answer (21) describes the modified cosmic Chaplygin black hole. As a result, we were able to fully determine the geometry of our desired black hole. We are now at a stage where we can study the thermodynamics of the system.

In this case, the mass of the black hole from equation (21) will be as follows

$$M = \frac{r_h}{l^2} + \frac{Q^2}{{r_h}^3} - \frac{D}{r_h} e^{\frac{r}{3}} \tag{23}$$

Then, using equations (11) and (23), we will have the temperature of system as follows

$$T = \frac{1}{4\pi}\left(\frac{3r_h}{l^2} - \frac{Q^2}{{r_h}^3} - \frac{4D}{3r_h} e^{\frac{r}{3}}\right) \tag{24}$$

The important question now is whether this physical system has thermodynamic stability or not. To understand this, we examine the specific heat in the constant volume of the system, which is obtained from the following equation

$$C_V = T\frac{dS}{dT} \tag{25}$$

According to this result, black holes in large radii have a positive specific heat and are stable, but with decreasing horizon radius, the specific heat is negative and the black hole is thermodynamically in an unstable phase. But to understand this instability more accurately, we need to look at quantum effects, which is not the subject of this article. Therefore, the black hole is stable in normal radii and we can conclude that its dual fluid, modified cosmic Chaplygin gas, also has thermodynamic stability.

6 Conclusion

In this paper, we consider a spherically symmetric black hole in AdS space and obtain its metric function using thermodynamic relations (the first law of thermodynamics) so that the desired black hole is changed like cosmic Chaplygin gas, which is a candidate for describe the nature of the dark energy in the universe. This black hole has two new parameters compared to the previously studied samples, which are the electric charge and the cosmic parameter. We can now consider the metric (5) with the answer (21) and study the thermodynamics of this black hole and obtain information about its phase transition and critical points.

By studying the behavior of specific heat at a constant volume of a black hole, we obtained information about its stability. We found that in the physical range (positive temperature) the black hole is in a stable phase, and we concluded that its dual fluid, which is modified cosmic Chaplygin gas, is also stable.

References

[1] Rajagopal, A., Kubiznak, D., Mann, R. B., 2014. "Van der Waals black hole". Phys. Lett. B737 (2014) 277

[2] Delsate, T., Mann, R. B., 2015. "Van Der Waals black holes in d dimensions". JHEP 1502 (2015) 070

[3] Upadhyay, S., Pourhassan, B., 2019. “Logarithmic corrected Van der Waals black holes in higher dimensional AdS space”. Prog. Theor. Exp. Phys. 2019 (2019) 013B03

[4] Cvetic, M., Gubser, S., 1999. "Phases of R-charged Black Holes, Spinning Branes and Strongly Coupled Gauge Theories". JHEP 9904 (1999) 024

[5] Niu, C., Tian, Y., Wu, X. -N., 2012. "Critical phenomena and thermodynamic geometry of Reissner-Nordstrom-anti-de Sitter black holes". Phys. Rev. D 85 (2012) 024017

[6] Sadeghi, J., Pourhassan, B., Rostami, M., 2016. "P-V criticality of logarithm-corrected dyonic charged AdS black holes". Phys. Rev. D 94 (2016) 064006

[7] Kubiznak, D., Mann, R. B., 2012. "P-V criticality of charged AdS black holes". JHEP 1207 (2012) 033

[8] Chaplygin, S., 1904. "On gas jets". Sci. Mem. Moscow Univ. Math. Phys. 21 (1904) 1–121

[9] Pourhassan, B., 2013. “Viscous Modified Cosmic Chaplygin Gas Cosmology”. Int. J. Mod. Phys. D 22 (2013) 1350061
[10] Debnath, U., 2020. "Thermodynamic black hole with modified Chaplygin gas as a heat engine". Eur. Phys. J. Plus. 135 (2020) 424
[11] Hawking, S.W., 1974. "Black hole explosions?". Nature 248 (1974) 30
[12] Hawking, S.W., 1975. "Particle creation by black holes". Commun. Math. Phys. 43 (1975) 199
[13] Bekenstein, J.D., 1974. "Generalized second law of thermodynamics in black-hole physics". Phys. Rev. D 9 (1974) 3292

Talk link: https://holography.du.ac.ir/en/files.php?rid=24

Wednesday 9th March 2022

Full paper – poster

Holographic dark energy from f(G) modified gravity perspective

S. Noori Gashti[1], J. Sadeghi[2], A. S. Sefiedgar[3]
[1]Department of Physics, Faculty of Basic Sciences, University of Mazandaran
P. O. Box 47416-95447, Babolsar, Iran
Email: saeed.noorigashti@stu.umz.ac.ir
[2] Department of Physics, Faculty of Basic Sciences, University of Mazandaran
P. O. Box 47416-95447, Babolsar, Iran
Email: pouriya@ipm.ir
[3] Department of Physics, Faculty of Basic Sciences, University of Mazandaran
P. O. Box 47416-95447, Babolsar, Iran
Email: a.sefiedgar@umz.ac.ir

Abstract. In this paper, we evaluate the cosmological implications of dark energy from a holographic perspective in the framework of a modified Gauss-Bonnet theory of gravity f(G) with respect to the Granda-Oliveros cut-off. Therefore, using holographic dark energy (HDE) and two forms of the scale factor, we reconstruct the f(G) model and study the different conditions such as energy conditions (WEC), (DEC), and (SEC) and show whether it is satisfactory or not. Also, we discuss the dynamic analysis of these models regarding the important tools as statefinder diagnostic (r, s). Finally, we study the stability of the two models and compare the results with the latest observable data.

Keywords: Holographic dark energy, Modified f(G) theory, Energy conditions,

1 Introduction

Recently various phenomena studied by researchers have been proven thanks to recent observations, such as the phenomenon of the accelerated universe, inflation, black holes [1, 2, 3, 4]. Since the nature of dark energy is still unknown, different models are considered for it and compared with the latest observable data. The simplest model that is a candidate for dark energy is ΛCDM. Also, other dynamic models are mentioned [3, 4]. Of course, determined to differentiate each dark energy model using the equation of state parameter $\omega = p_{eff} / \rho_{eff}$. So far, various candidates for dark energy introduced in the literature, and recent efforts have led to the introduction of many newer models that are compatible with the latest observable data and cosmic phenomena [3]. As mentioned, recent observations have been made through SNe Ia, indicating that a number of these dynamic models are more compatible with recent cosmic phenomena than the constant cosmological model Λ-Dark energy, despite its unknown nature, has always been deeply analyzed [5]. One of the most important dynamic models of dark energy is called (HDE), which researchers have recently considered and evaluated from a different perspective. Its cosmological implications have also been studied [6]. Dynamic models of dark energy studied in various types of structures, including the modified theories of gravity, which play a very important role for the late acceleration of the universe [4]. Researchers deeply considered modified theories also include different types such as f(R) gravity, f(R, t) gravity, f(T) gravity, braneworld models, Gauss-Bonnet gravity, and Galileon gravity, in various types of cosmic studies. The ones used the modified scalar-Gauss-Bonnet theory of gravity in many cosmology studies and investigated its cosmological implications. Scalar-Gauss-Bonnet gravity in form f(G) in [7] has been introduced. This theory also somehow describes the acceleration of the universe and the different periods of radiation/matter-dominated eras, which by Myrzalulov [8] checked out. In [10], They considered different and specific forms of theory f (G) and examined inequalities concerning different energy conditions, and showed the viability of different forms of f (G) theory. Now we will study different implications in the structure of the modified f(G) gravitational and the structure of HDE theory with respect to the Granda-Oliveros cut-off.

2 HDE & f(G) gravity

This section will first review the modified theory of gravity f(G) and then discuss the HDE structure and the reconstruction of our theory. The action of a modified theory of f(G) gravity in which Einstein's gravity coupled with a perfect fluid concerning the structure of Gauss-Bonnet term is described as $S = \int d^4x \sqrt{-g}\,(\frac{1}{2k^2} R + f(G) + Lm)$ [11]. According to this equation, $G = R^2 - 4R_{\mu\nu}R^{\mu\nu} + R_{\mu\nu\lambda\sigma} R^{\mu\nu\lambda\sigma}$, $k^2 = 8\pi G$, R, $R_{\mu\nu}$, $R_{\mu\nu\lambda\sigma}$ and g determine the Ricci scalar curvature, Ricci curvature tensor, Riemann curvature tensor and metric tensor $g_{\mu\nu}$, respectively. Also, in the above equation, the parameter Lm represents the Lagrangian of the matter present. The variation of this equation with respect to a parameter $g_{\mu\nu}$ called the metric tensor leads to the field equations as follows.

$$1/2k^2 (-R^{\mu\nu} + 1\ 2\ g^{\mu\nu} R) + T^{\mu\nu} + 1\ 2\ g^{\mu\nu} f(G) - 2f_G R R^{\mu\nu} + 4f_G R^{\mu}{}_{\rho} R^{\nu\rho} - 2f_G R^{\mu\rho\sigma\tau} R^{\nu}{}_{\rho\sigma\tau} - 4f_G R^{\mu\rho\sigma\nu} R_{\rho\sigma} + 2(\nabla^{\mu}\nabla^{\nu} f_G)\, R - 2g^{\mu\nu}(\nabla^2 f_G) R - 4(\nabla_{\rho}\nabla^{\mu} f_G) R^{\nu\rho} - 4(\nabla_{\rho}\nabla^{\nu} f_G) R^{\mu\rho} + 4(\nabla^2 f_G) R^{\mu}{}_{\nu} + 4g^{\mu\nu}(\nabla_{\rho}\nabla_{\sigma} f_G) R^{\rho\sigma} - 4(\nabla_{\rho}\nabla_{\sigma} f_G) R^{\mu\nu\rho\sigma} = 0 \tag{1}$$

In the above equation, $f_G = df/dG$ and the two functions f and $T_{\mu\nu}$ specify the energy-momentum tensor of the perfect fluid, respectively. But in this paper, we have a special form of gravitational f (G) mentioned in [11]. We suffice and continue the equations with this form of f(G). In general, the two parameters $R = 6(dH/dt + 2H^2)$ and $G = 24H^2 (dH/dt + H^2)$, which determine the Ricci scalar curvature and Gauss-Bonnet invariant in spatially flat FRW space-time. The spatially homogeneous space FRW mentioned above is specified as $ds^2 = -dt^2 + a^2(t)(dx^2 + dy^2 + dz^2)$. Where a(t) is the scale factor. In these above equations, the dot is a time derivative. According to the above explanation, the first equation of FRW concerning $8\pi G = 1$ is in the following form.

$$H^2 = 1/3\,(G f_G - f(G) - 24 dG/dt\, H^3 f_{GG} + \rho_m) = 1/3\,(\rho_G + \rho_m) \tag{2}$$

where $f_{GG} = d^2 f/dG^2$. The subscripts (m) in the equations represent matter's contribution in each of the quantities of energy density and pressure. We now present a reconstructed scheme for studying gravity f(G) in a holographic dark energy structure with a Granda-Oliveros cut-off. The holographic energy, as well as the Granda-Oliveros cut-off (L_{GO},) are shown as follows [19].

$$\rho_\Lambda = 3/L^2_{GO}, \qquad L_{GO} = (\delta\, dH/dt + \lambda H^2)^{-1/2} \tag{3}$$

λ and δ are constant parameters in the above equation. Dimensionless DE density can obtain according to energy density ρ_Λ of dark energy and critical energy density $\rho_{cr} = 3H^2$; $\Omega_\Lambda = \rho_\Lambda / \rho_{cr} = c^2 / L^2_{GO} H^2$. The equation of state parameter is as $\omega_{eff} = p_{eff} / \rho_{eff}$. So,

$$\rho_{eff} = \rho + 1/2k^2 \left(- f(G) + 24H^2 (H^2 + dH/dt) f_G\right) \quad (4)$$

$$p_{eff} = p + 1/2k^2 \left(f(G) - 24H^2 (H^2 + dH/dt) f_G + 8(24)H^2 (6[dH/dt]^3 + 6H dH/dt\, d^2H/dt^2 + 24H^2 (dH/dt)^2 + 6H^3 d^2H/dt^2 + 8H^4 dH/dt + H^2 d^3H/dt^3) f_{GG} + 8(24)^2 H^4 (2H^2 + H d^2H/dt^2 + 4H^2 dH/dt)^2 f_{GGG}\right) \quad (5)$$

Setare in [13] examines such a reconstruction about the modified gravitational f(R) model in the framework of HDE, and we somehow study such a structure in the case of the modified gravitational f(G) model concerning two different models of the scale factor. Now concerning the energy density of f(G) gravity in equation (2) and energy density of HDE model in equation (3) will lead to the following differential equation [9]

$$24H^3 (dG/dt)^{-1} d^2f(G)/dt^2 - (24H^3 (dG/dt)^{-2} d^2G/dt^2)\, df(G)/dt + f(G) = -3(\delta\, dH/dt + \lambda H^2) \quad (6)$$

3 Model I

As shown in the reconstruction of f(G) gravity in equation (10), investigating is very difficult to solve this equation analytically. Therefore, we prefer the numerical solution for this gravitational model, so that we introduce two scale factors and then examine the modified f(G) gravity structure in the HDE framework. Hence the first ansatz of the scale factor model, a hybrid model, is expressed in the following form.

$$a(t) = (t_\sigma - t)^n \exp(t) \quad (7)$$

where t_σ and n are constant parameters. According to the above ansatz, we consider the hybrid form $t^n \exp(t)$. By selecting this scale factor and explaining it in the previous section, we can easily calculate quantitative values as H and G, as follows. $H = (n + t)/t$ and $G = (24(n + t)^2 ((-1+n)n+2nt+t^2))/t^4$. Observing a constraint on the form $\lim_{G\to 0} f(G) = 0$ indicates that the above reconstructed model has sufficient conditions to validate that the HDE f(G) model is a realistic model. Hence, the reconstruction of the f(G) model given in the above equations shows the compatibility of the modified theories of gravity with HDE.

4 Model II

We introduce another ansatz of scale factor and follow the same process as before.
Hence, the new model is expressed in the following form.

$$a(t) = \beta\, t \exp(\alpha n t) \quad (8)$$

where n, α and β are constant parameters. Now we can easily calculate quantitative values as H and G as follows, $H = \alpha n + 1/t$ and $G = (24\alpha n (1 + \alpha n t)^2 (2 + \alpha n t))/t^3$. Also, to calculate functions and plot them, we used numerical methods to solve problems that may cause difficulties in calculating and plotting analytical figures.

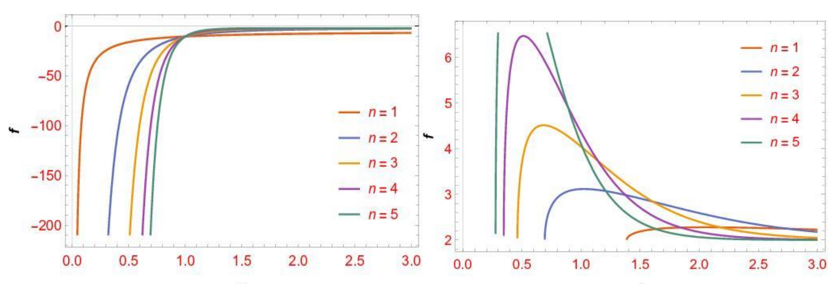

Figure 1. The plan of f(G) in terms of t in fig (1a) for model I and in fig (1b) for model II, according to the different values of n and constant parameters $\alpha = \beta = 0.1$, $\lambda = 1.5$ and $\delta = 1$

We plotted the changes of the modified f(G) gravitational model in the HDE structure for the model I in figure (1a) and model II in figure (1b) in terms of variables t according to the constant parameters $\alpha = \beta = 0.1$, $\lambda = 1.5$ and $\delta = 1$ respectively. As mentioned in the text, the increased values of f(G) are related to the increase of the parameter t, and finally it converges zero value. For the second model, changes occur in proportion to time passage. For different constant parameters as shown in the figure on the right, first an increase occurs, and then the figure takes a decreasing direction. These conditions can ensure for HDE f(G) theory as a realistic model.

5 Energy condition of I and II

Different types of these energy conditions such as (NEC), (WEC), (DEC), and (SEC) can be named, which obtained in a special form through the Raychaudhuri equation [10] also in different scenarios, such as the evolution of the deceleration parameter, phantom field potential, and an expansion scenario of the universe [12]. About different energy conditions, NEC and the WEC are very important despite their simplicity. Dissatisfaction or violation of the NEC energy condition will lead to the violation of other energy conditions, so it is important. This issue guarantees the second law of thermodynamics and indicates a decrease in energy density during the accelerating expansion of the universe. Violation (SEC) also indicates the rapid expansion of the universe. In general, can describe the different energy conditions for the mentioned theory in the following form. [10], $NEC = \rho_{eff} + p_{eff} \geq 0$, $WEC = \rho_{eff} \geq 0$, $\rho_{eff} + p_{eff} \geq 0$, $DEC = \rho_{eff} \geq 0$, $\rho_{eff} \pm p_{eff} \geq 0$, $SEC = \rho_{eff} + 3p_{eff} \geq 0$, $\rho_{eff} \pm p_{eff} \geq 0$. We can determine the energy conditions for the first model using equations (4), (5) and (7) and for the second model with the equations (4), (5) and (8). After calculating these energy conditions, it is possible to determine the satisfaction or violation of energy conditions by plotting some figures. We show the energy conditions for model (I) in figure (2a) and model (II) in figure (2b, 2c, 2d) for mentioned constant values and parameters. In Figure (2), the NEC energy conditions for the two models violated except will be satisfactory for model II for the even values of n. Also, the condition of violation or satisfaction of these cases is clear. But, in all cases, except for the even n in model II, the SEC is violated. Its violation is a confirmation of the accelerated expansion of the universe.

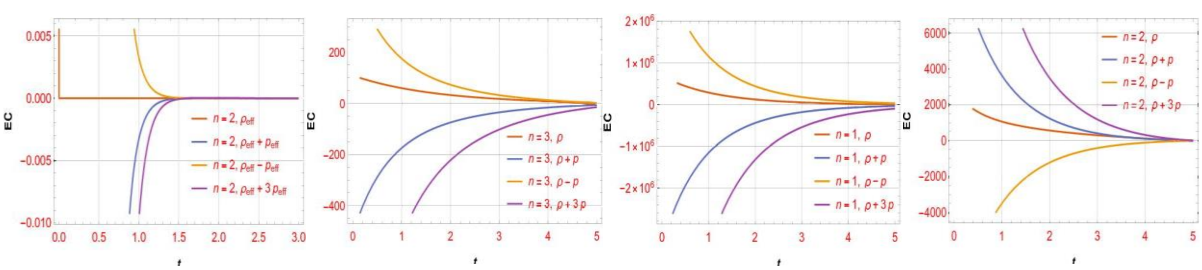

Figure 2. The plot of EC in terms of t in fig (2a) for model I and in fig (2b, 2c, 2d) for model II, according to the different values of n and constant parameters $\alpha = \beta = 0.1$, $\lambda = 1.5$, $\delta = 1$

6 Stability of I and II

Now we want to check the stability of our mentioned model with the help of sound speed. Hence, we will have. $C_s^2 = (dp_\Lambda/dt) / (d\rho_\Lambda/dt)$. As it is clear from the above equation, the sign of the above equation is very important because the negative or positive of the above equation indicates the stability or instability of the models. The negative value of the above equation indicates the classical instability of a certain perturbation in general relativity [14, 15]. A very important point about the speed of sound in the HDE structure is that there must always be a negative value in the future event horizon as IR cutoff [15]. However, for two forms, Chaplygin gas and tachyon, a non-negative value is observed. Researchers also investigate the sound speed in agegraphic DE structures. It has a negative value, which leads to perfect fluid instability for the model. [14] Also, one studied Various structure such as the ghost QCD DE model in this field, which shows the system's instability. Here we plot the speed of sound in terms of cosmic time for two models. The figures show that sound speed values for both present and future times are negative, depicting classical instability for both models. In other words, the modified f (G) gravitational model in the HDE structure is classically unstable for both scale factor models.

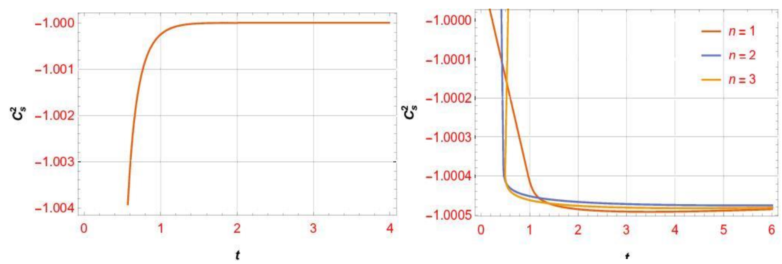

Figure 3. The plot of C^2_s in terms of t and n = 2 in fig (3a) for model I and in fig (3b) for model II, according to the different values of n and constant parameters α = β = 0.1

7 Statefinder diagnostic

It has often been difficult to distinguish between different models for dark energy. So, for solving this problem, the ones used a diagnostic pair (r, s) statefinder in [16, 17] as $r = (da/dt)^3/aH^3$ and $s = (r-1)/3(q-½)$. These equations show that the decelerating parameter $q = -(d^2a/dt^2)/(aH^2)$ and the Hubble parameter is as $H = (da/dt)/a$. This powerful tool deals with the first to third derivatives of the scale factor and shows the geometric properties of dark energy. We can name earlier interesting work, including studying modified HDE in the Kaluza-Klein universe, two dark energy models with powerful diagnostic tools (Panotopoulos), and different forms of dark energy in the Kaluza-Klein universe. [18]. This diagnostic tool distinguishes between a wide range of dark energy in different states such as the cosmological constant, Chaplygin gas, quintessence, braneworld models, the interacting DE, etc. [16]. We know that the constant point of the pair r = 1, s = 0 indicates the standard model of dark energy, i.e. (Λ-Cold-dark-mater), which the mentioned models can reach and passing it. It means that these models can reach this phase of the universe. Figure (4) also shows the changes of two very important parameters of the powerful diagnostic tool (r – s) for both models. As it is clear, the changes of {r − s} trajectories are shown for the model I in figure (4a) and model II in figure (4b) for various values of constant parameters as n. As it is clear in both models, {r − s} trajectories reach the constant points related to the Λ-CDM model with the specification (r = 1, s = 0) and pass it well. It is a kind of indication that this structure is reconstructed for different values considered for constant parameters. According to both models mentioned in the text, it can reach the Λ-CDM phase of the universe

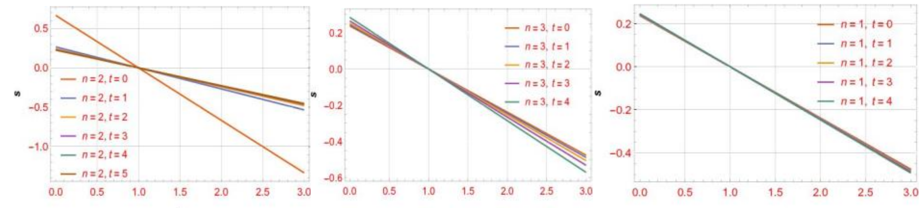

Figure 4. The plot of s in terms of r in fig (4a) for model I and in fig (4b,4c) for model II, according to the constant parameters $\alpha = \beta = 0.1$, $\lambda = 1.5$ and $\delta = 1$

8 Conclusions

In this paper, we evaluated some cosmological implications of dark energy from a holographic perspective concerning various form factor scales, i.e., $t^n \exp(t)$, $\beta t \exp(\alpha n t)$ and in the framework of a modified Gauss-Bonnet theory of gravity; f(G) with respect to the Granda-Oliveros cut-off. Therefore, using holographic dark energy (HDE) and two different forms of the scale factor, we reconstructed the f(G) model and studied the different conditions of these models. Also, by defining effective energy density ρ_{eff} and pressure p_{eff}, we investigated different energy conditions EC such as (WEC), (DEC), and (SEC) and show whether it is satisfactory or not. Also, we examined the behavior of the equation of state (EoS) using the two parameters ρ_{eff} and p_{eff} and the other constant parameters. Then we discussed the dynamic analysis of these models regarding the important tools as statefinder diagnostic (r, s). Finally, we studied the stability of the two models and compared the results with the latest observable data. Of course, an important issue that can focus on in future work is to study the different conditions of the swampland program, such as the refined swampland conjecture and TCC.

References

[1] D. N. Spergel et al., Astrophys. "First-Year Wilkinson Microwave Anisotropy Probe (WMAP)* Observations: Determination of Cosmological Parameters" J. Suppl. 148 (2003) 175

[2] S. Perlmutter et al., "Measurements of Ω and Λ from 42 High-Redshift Supernovae Astrophys. J. 517 (1999) 565

[3] E. J. Copeland, M. Sami and S. Tsujikawa, "Dynamics of dark energy" Int. J. Mod. Phys. D 15 (2006) 1753

[4] S. Tsujikawa, "Modified gravity models of dark energy" Lect. Notes Phys. 800 (2010) 99

[5] M. Li et al., "Dark energy" Commun. Theoret. Phys. 56 (2011) 525

[6] Shuang Wang, Yi Saeed Pourojaghi, and Mohammad Malekjani,"A new comparison between holographic dark energy and standard Λ -cosmology in the context of cosmography method'' The Euro. Phys. J C81 (2021) 575

[7] S. Nojiri and S. D. Odintsov, "Modified Gauss–Bonnet theory as gravitational alternative for dark energy " Phys. Lett. B 631 (2005) 1

[8] R. Myrzakulov, D. Sez-Gmez and A. Tureanu, "On the Λ CDM Universe in f (G) gravity" Gen. Relativ. Gravit. 43 (2011) 1671

[9] S. Nojiri, and S. D. Odintsov, "Introduction to modified gravity and gravitational alternative for dark energy" Int. J. Geom. Meth. Mod. Phys. 4 (2007) 115

[10] N. M. Garcia, T. Harko, F. S. N. Lobo and J. P. Mimoso, "Energy conditions in modified Gauss-Bonnet gravity" Phys. Rev. D 83 (2011) 104032

[11] S. Nojiri and S. D. Odintsov, "Modified Gauss–Bonnet theory as gravitational alternative for dark energy" Phys. Lett. B 631 (2005) 1

[12] A. A. Sen and R. J. Scherrer, "The weak energy condition and the expansion history of the Universe" Phys. Lett. B 659 (2008) 457

[13] M. R. Setare, “Holographic modified gravity” Int. J. Mod. Phys. D 12 (2008) 2219
[14] K. Y. Kim, H. W. Lee and Y. S. Myung, “Instability of agegraphic dark energy models” Phys. Lett. B 660 (2008) 118
[15] K. Y. Kim, H. W. Lee and Y. S. Myung, “Instability of agegraphic dark energy models” Phys. Lett. B 660 (2008) 118
[16] Y. S. Myung, “Instability of holographic dark energy models” Phys. Lett. B, 652 (2007) 223
[17] Vandna Srivastavaab UmeshKumar Sharma, “Statefinder hierarchy for Tsallis holographic dark energy” New Astronomy 78 (2020) 101380
[18] V. Sahni, A. Shafieloo, and A. A. Starobinsky, “Two new diagnostics of dark energy” Phys. Rev. D 78 (2008) 103502
[19] M. Sharif, and A. Jawad, “Modified holographic dark energy in non-flat Kaluza–Klein universe with varying G” Europ. Phys. J. C 72 (2012) 1901
[20] M.R. Setare, “Holographic modified gravity” Int. J. Mod. Phys. D 12 (2008) 2219

Talk link: https://aparat.com/v/NIkox

Wednesday 9th March 2022

Full paper – Oral

Dirac form factor of the n+γ*→r(1535) transition in the hard-wall AdS/QCD model

Sh.A.Mamedov [1], Sh.I.Taghiyeva[2],
[1] Institute for Physical Problems, Baku State University, Baku, Azerbaijan,
[1] Theoretical Physics Department, Physics Faculty, Baku State University, Baku, Azerbaijan,
[1] Instutute of Physics, Azerbaijan National Academy of Sciences, Baku, Azerbaijan.
Email: sh.mamedov62@gmail.com
[2] Theoretical Physics Department, Physics Faculty, Baku State University, Baku, Azerbaijan,
Email: shahnaz.ilqarzadeh.92@mail.ru

Abstract. We define Dirac form factor N+γ^*→R(1535) transition for N* with negative parity within hard-wall AdS/QCD model. Using AdS/CFT correspondence between generating functions in the bulk and boundary theories, we obtain an expression for the Dirac form factor from the bulk interaction action. We plot the form factor dependence from the transferred momentum square using MATHEMATICA package.

Keywords: AdS/CFT correspondence, Roper nucleon, form factor.

1 Introduction

The study of electromagnetic properties of Roper resonance, open new opportunities for understanding the structure of hadrons. Nucleon resonances have been discussed in the soft-wall AdS/QCD model, Light Front holography, covariant spectator quark model in Refs. [1,3-5]. In Ref. [1] authors apply the Light Front holography in the soft wall approximation to the study of the electromagnetic structure of the nucleon and nucleon excitations. In Ref. [2] authors predict the transition form factors and the helicity amplitudes using covariant spectator quark model for have also been discussed in the AdS soft-wall approach at finite temperature in Ref. [6]. In this work, we discuss N+γ*→R(1535) transition Dirac form factor for N* with negative parity within hard-wall AdS/QCD model.

The article is organized as follows. In Sec. II we briefly review the hard-wall model in AdS/QCD. In Sec. III we present a vector field in the AdS space. In Sec. IV we calculate and discuss the Dirac form factor for the N+γ*→R(1535) reaction. Finally, in Sec. V we present our numerical result for this form factor.

2 The hard-wall model of ADS/QCD

In this section, we present profile functions for a nucleon in the framework of the hard-wall AdS/QCD model. The bulk action for a Dirac spinor (and similarly for N_2) is written:

$$S_N = \int d^5x\sqrt{g}\left\{\frac{i}{2}\overline{N}_1 e_A^M \Gamma^A \nabla_M N_1 - m_5 \overline{N}_1 N_1 + (1 \leftrightarrow 2 \& m_5 \leftrightarrow -m_5)\right\}, \tag{1}$$

where, $e_A^M = \frac{1}{z}\eta_M^A$ is the vielbein, m_5 is the mass of the bulk spinor, $N_i = N_{iL} + N_{iR}$ have defined with the properties $i\Gamma^5 N_{1L} = N_{1L}$, $i\Gamma^5 N_{1R} = -N_{1R}$ and Γ^A*(A=0,1,2,3,5)* are the the Dirac matrices. The gauge and Lorentz-covariant derivative is defined as:

$$\nabla_M = \partial_M - \frac{i}{4}\omega_M^{AB}\Sigma_{AB} - i(A_L^a)_M t^a \tag{2}$$

Here ω_M^{AB} is spin connection [3, 7] and its non-vanishing components are given by:

$$\omega_M^{5A} = -\omega_M^{A5} = \frac{1}{z}\delta_M^A. \tag{3}$$

Taking a variation from the (1) action with respect to $\overline{N}_1$ and applying the least action principle, one obtains a following equation with the boundary conditions:

$$(ie_A^M\Gamma^A\nabla_M - m_5)N_1 = 0, \tag{4}$$

$$[\delta\overline{N}_1 e_A^5\Gamma^A N_1]_\epsilon^{z_m} = 0. \tag{5}$$

Fourier-transform of the bulk spinor is:

$$N_{1L,R}(x,z) = \int d^5p\, f_{1L,R}(p,z)\Psi_{1L,R}(p)e^{-ipx} \tag{6}$$

where $\Psi_{1L,R}(p)$ obey 4D Dirac equation

$$\gamma^\mu p_\mu \Psi_{1L,R}(p) = |p|\Psi_{1R,L}(p) \tag{7}$$

And $f_{1L,R}$ satisfy equations over the z variable [8]:

$$\left(\partial_z - \frac{2+m_5}{z}\right)f_{1L} = -|p|f_{1R}, \tag{8}$$

$$\left(\partial_z - \frac{2-m_5}{z}\right)f_{1R} = |p|f_{1L}. \tag{9}$$

Eliminating f_{1R} from the (8) and (9) equations the equation for the f_{1L} profile function can be found:

$$(\partial_z^2 - \frac{4}{z}\partial_z + \frac{6+m_5-m_5^2}{z^2})f_{1L} = -p^2 f_{1L}. \tag{10}$$

Similarly, we have for the f_{1R} profile function:

$$(\partial_z^2 - \frac{4}{z}\partial_z + \frac{6+m_5-m_5^2}{z^2})f_{1R} = -p^2 f_{1R}. \tag{11}$$

Near the UV boundary, $z = \epsilon$, the $f_{1L,R}$ profile functions are given by [3,8]:

$$f_{1L} \cong c_1(1+2m_5)z^{2+m_5} + c_2|p|z^{3-m_5}, \tag{12}$$

$$f_{1R} \cong c_2(2m_5-1)z^{2-m_5} + c_1|p|z^{3+m_5}. \tag{13}$$

$c_{1,2}$ are the normalization constants, which was found in [4] and are equal to:

$$|C_{1,2}^n| = \frac{\sqrt{2}}{z_m\, \mathcal{J}_2(m_n z_m)}. \tag{14}$$

The normalizable solutions for nonzero modes are given by:

$$f_{1L,R}(p,z) \sim z^{5/2} J_{m_5 \mp (1/2)}(|p|z)$$

3 Vector field in ads space

The action in the five-dimensional AdS space for vector field will be written as follows:

$$S = \int d^5 x \sqrt{g} Tr\left(-\frac{1}{2g_5^2} F_{MN}^2\right), \tag{15}$$

where, g is the determinant of metric tensor g_{MN}, g_5 is related to the number of colors N_c ($g_5^2 = \frac{12\pi^2}{N_c}$), $F_{MN} = \partial_M V_N - \partial_N V_M - i[V_M, V_N]$ is vector field strength tensor. Transverse part of vector field will be written as $V_{\perp\mu}(q,z) = V(q,z) V_\mu^0(q)$ and the equation of motion obtained from the (15) action gives an equation for the $V(q,z)$ profile function [5]:

$$\left(z\partial_z\left(\frac{1}{z}\partial_z V(q,z)\right) + q^2 V(q,z)\right)_\perp = 0 \tag{16}$$

The equation (16) will be solved under the $V(q,\varepsilon) = 1$ and $\partial_z V(q, z = z_m) = 0$ ultraviolet (UV) and infrared (IR) boundary conditions, respectively. Solution is expressed in terms of the first kind Bessel functions:

$$V(q,z) = \frac{\pi}{2} zq\left(\frac{Y_0(qz_0)}{J_0(qz_0)} J_1(qz) - Y_1(qz)\right). \tag{17}$$

4 Dirac form factor of the N+Γ*→R(1535) transition

In general, the action for interaction is written as follows:

$$S_{int} = \int d^4 x dz \sqrt{g} L_{int}(x,z) \tag{18}$$

where, $L_{int}(x,z)$ is the interaction Lagrangian and it is given by following terms [5]:

$$L_{int}(x,z) = \sum_{i=+,+;\tau} c_\tau^{RN} \bar{\psi}_{i,\tau}^R(x,z) \hat{V}_i(x,z) \psi_{i,\tau}^N(x,z) \tag{19}$$

$$\hat{V}_\pm(x,z) = \tau_3 \Gamma^M V_M(x,z) \pm \frac{i}{4} \eta_V [\Gamma^M \Gamma^N] V_{MN}(x,z) \tag{20}$$

Here c_τ^{RN} is the set of parameters, which mix the contributions of the AdS fermion fields with the different twist dimension, $V_{MN}(x,z)$ is defined as: $V_{MN} = \partial_M V_N - \partial_N V_M$, τ_3 is the Pauli matrix, $\eta_V = diag(\eta_p, \eta_n)$.

According to AdS/CFT correspondence, the action for the four-dimensional field theory is equal to the classical action for the five-dimensional AdS theory [10,11]:

$$Z_{4D}[\phi^0] = Z_{AdS}[\phi^0] = \exp(iS_{5D}[\phi_{cl}]) \tag{21}$$

The vacuum expectation of the nucleon's vector current can be defined by taking variation from the generating functional Z_{AdS} of the bulk theory:

$$< J_\mu >= -i \frac{\delta Z_{AdS}}{\delta \hat{V}^0} |_{\hat{V}^0=0}, \tag{22}$$

The electromagnetic transition between nucleon and resonance can be described by the current [4]:

$$J^\mu = \bar{u}_f(P_f)\left[\gamma_\mu^T F_1^{fi}(Q^2) + \frac{1}{m_{fi}} \sigma_{\mu\nu} Q_\nu F_2^{fi}(Q^2)\right] u_i(P_i), \tag{23}$$

where, $u_i, \bar{u}_f$ are Dirac spinors, $m_{fi} = (m_f + m_i)$, $F_1^{fi}(Q^2)$, $F_2^{fi}(Q^2)$ are called Dirac and Pauli form factors, respectively. Dirac form factor will be found from the comparison of the two currents (22) and (23):

$$F_1^{fi}(Q^2) = G_1(Q^2) + g_V G_2(Q^2) + \eta_p G_3(Q^2) \tag{24}$$

and $G_i(Q^2)$ have an expression:

$$G_1(Q^2) = \frac{1}{4}\int_0^{z_m} dz c_\tau^{RN} V(Q,z)(f_L(z)\, f_L^*(z) + f_R^*(z) f_R(z)).$$

$$G_2(Q^2) = \frac{1}{4}\int_0^{z_m} dz c_\tau^{RN} V(Q,z)(f_R(z)\, f_R^*(z) - f_L^*(z) f_L(z)).$$

$$G_3(Q^2) = \frac{1}{4}\int_0^{z_m} dz z c_\tau^{RN} \partial_z V(Q,z)(f_L(z)\, f_L^*(z) - f_R^*(z) f_R(z)).$$

6 Conclusions

As was noted in the introduction, the $N + \gamma^* \to R(1535)$ reaction was studied within several models[17]. In the present work, we apply the AdS/CFT holography in the hard wall approximation to the study of the electromagnetic structure of the nucleon and nucleon excitations. Finally, the free parameter are fixed as:

$$g_V = 1, \qquad \eta_p = 0.45,$$

$$c_3^{RN} = 0.72\,, \qquad \eta_n = -0.279.$$

Our numerical results for the $N + \gamma^* \to R(1535)$ transition Dirac form factor is presented in Fig.1 and we also include CLAS [13], MAID [14,15] and JLab/Hall C [16] experimental data, for a comparison in Fig.1. Our result is compatible with experimental data in the region $Q^2 > 1{,}5$.

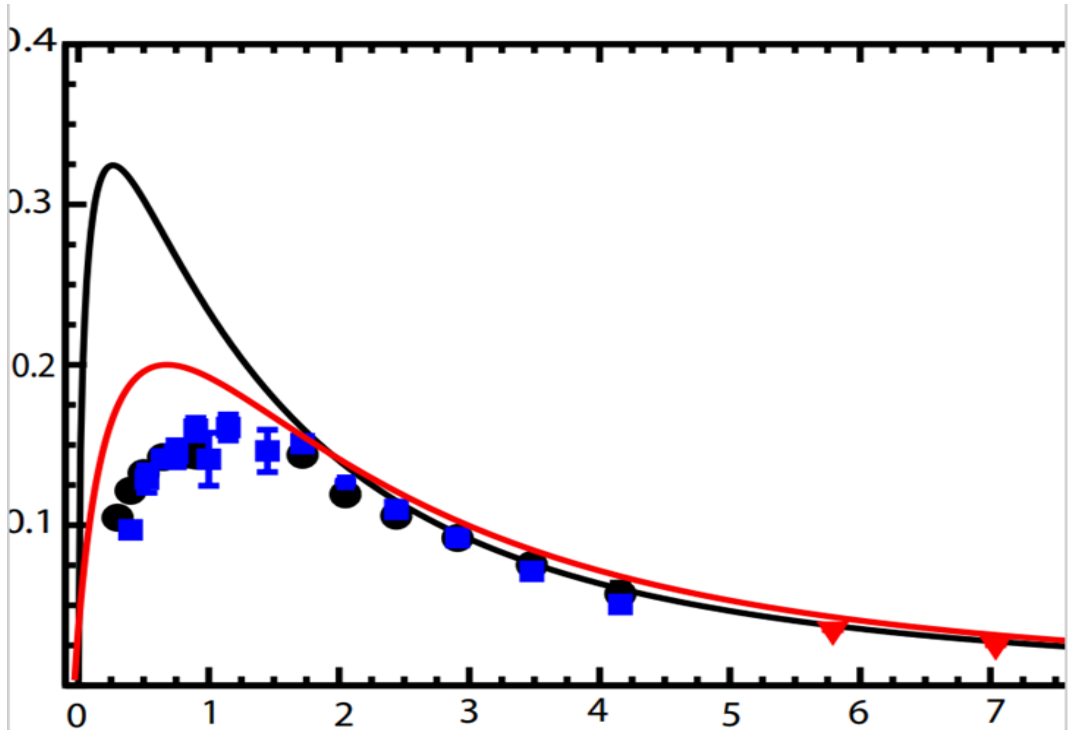

FIG. 1: Results for the $N + \gamma^* \to R(1535)$ transition Dirac form factor obtained by the hard-wall model (red thick solid line), given by the semirelativistic appoximation.(black thick solid line) [17]. Data from CLAS [13] (full circles), MAID [14,15] (full squares), JLab/Hall C [16] (triangles).

References

[1] G. Ramalho, Phys. Rev. D 96 (2017) 054021
[2] G. Ramalho, K. Tsushima, Phys. Rev. D 89 (2014) 073010
[3] Th. Gutsche, V. E. Lyubovitskij and I. Schmidt, Phys. Rev. D 97 (2018) 054011
[4] Sh. Mamedov, B. B. Sirvani, I. Atayev, N. Huseynova Int.J.Theor.Phys. 56 (2017) 1861
[5] Th. Gutsche, V. E. Lyubovitskij, I. Schmidt and A. Vega, Phys. Rev. D 87 (2013) 016017
[6] Th. Gutsche, V.E. Lyubovitskij, I. Schmidt, Nuc. Phys. B 952 (2020) 114934

[7] H.Ch. Ahn, D.K. Hong, Ch. Park and S. Siwach, Phys.Rev. D 80 (2009) 054001

[8] D.K. Hong, T. Inami, H.U. Yee, Phys. Let. B 646 (2007) 165

[9] Ch. Chen, Y. Lu, D. Binosi, C.D. Roberts, J.R. Quintero, J. Segovia, Phys. Rev. D 99 (2019) 034013
[10] C.E. Carlson, arxiv:0809.4853v1 [hep-ph] 28 Sep. 2008,
[11] H. Nastase, "Introduction to AdS/CFT", arXiv:0712.0689 [hep-th]

[12] M.M. Ammon, Gauge/Gravity Duality applied to Condensed Matter Systems, Munchen 2010,
[13] I.G. Aznauryan et al. [CLAS Collaboration], Phys. Rev. C 80 (2009) 055203

[14] D. Drechsel, S.S. Kamalov and L. Tiator, Eur. Phys. J. A 34 (2007) 69
[15] L. Tiator, D. Drechsel, S.S. Kamalov and M. Vanderhaeghen, Chin. Phys. C 33 (2009) 1069
[16] M. M. Dalton et al., Phys. Rev. C 80 (2009) 015205
[17] G. Ramalho, Phys. Rev. D 95 (2017) 054008

Talk link: https://aparat.com/v/bnvRO

Thursday 10th March 2022

Full paper – Oral

η/s for AdS Dilaton Black Brane

Mehdi Sadeghi
Department of Physics, School of Sciences, Ayatollah Boroujerdi University, Boroujerd, Iran
Email: Mehdi.sadeghi@abru.ac.ir

Abstract. We calculate the ratio of shear viscosity per entropy density for a dilaton black brane in AdS spacetime. There is a well- known conjecture that this ratio should be larger than η/s≥1/4π and we will show that this bound is saturated in this black brane.

Keywords: Shear viscosity, Entropy density, Fluid/Gravity duality

1 Introduction

AdS/CFT duality introduced by Maldacena [1] relates two kinds of theories: gravity in (n+1)-dimension and field theory in n-dimension. The most familiar example, the AdS/CFT duality asserts that SYM $\mathcal{N}=4$ Super Yang-Mills (SYM) theory is dual to Type IIB string theory on $AdS_5 \times S^5$. There's no way to solve the strongly coupled field theories either analytically or perturbatively. AdS/CFT duality is a technique to overcome this problem. By using this duality, we can translate the strongly coupled field theory into a weakly gravitational theory and vice versa. The map between these two different theories is known as holographic dictionary. In the long wavelength limit this duality leads to fluid/gravity duality. Any fluid is characterized by some transport coefficients. These coefficients identify the underlying microscopic properties of fluids which in turn rooted in the field theory interactions at strong coupling. So, the gauge/gravity duality would be a proper tool to calculate these coefficients. In this work, our interest is the shear viscosity, one of the transport coefficients. The conservation of energy and momentum in relativistic Hydrodynamics is as follows,

$$\nabla_\mu T^{\mu\nu} = 0 \tag{1}$$
$$T^{\mu\nu} = (\varepsilon + p)u^\mu u^\nu + p g^{\mu\nu} \tag{2}$$

Note that the term "relativistic fluid" doesn't mean the fluid is necessarily moves near the speed of light. However, the Lorenz symmetry preserves in the relativistic fluid.

We introduce a parameter expansion $\varepsilon = \frac{\ell_{mfp}}{L}$, where ℓ_{mfp} and L are the mean free path and the characterized length of system or the scale for the field fluctuations, respectively. The scale of field variations has to be large compared to the mean free path, $\ell_{mfp} \ll L$ for the validity of hydrodynamics regime on the boundary. We know that the regime where the fluid is valid corresponds to a theory with large AdS black holes. We can expand the energy-momentum tensor in terms of ε when it is $\varepsilon \ll 1$ [1-3]

$$T^{\mu\nu} = (\varepsilon + p)u^{\mu}u^{\nu} + pg^{\mu\nu} - \sigma^{\mu\nu} \tag{3}$$

$$\sigma^{\mu\nu} = P^{\mu\alpha}P^{\nu\beta}[\eta\left(\partial_{\alpha}u_{\beta} + \partial_{\beta}u_{\alpha} - \frac{2}{3}g_{\alpha\beta}\partial_{l}u^{l}\right) + \xi g_{\alpha\beta}\partial_{l}u^{l} \tag{4}$$

where η and ξ are shear and bulk viscosities, respectively.
In this article, we calculate shear viscosity by Green-Kubo formula,

$$\eta = -\lim_{\omega\to 0}\frac{1}{\omega}\mathrm{Im}G^{R}_{ij,ij}(\omega, 0) \tag{5}$$

Where $G^{R}_{ij,ij}(\omega, 0)$is as follows,

$$G^{R}_{ij,ij}(\omega, 0) = \int dtd\boldsymbol{x}e^{i\omega t}\theta(t)\langle[T_{ij}(t, \boldsymbol{x}), T_{ij}(0, \mathbf{O})]\rangle \tag{6}$$

In the following section, we review the dilaton black brane in AdS space-time. Then calculate the shear viscosity to the entropy density ratio and find out that it satisfies the conjectured bound $\frac{1}{4\,\pi}$.

2 Dilaton Black Brane Solution

We consider the 5-dimensional theory in which gravity is coupled to dilaton and Maxwell field with an action [4],

$$S = \int d^{5}x\sqrt{-g}(\,R - 2\Lambda - \frac{4}{3}\partial_{\mu}\phi\partial^{\mu}\phi - V(\phi) - e^{-\frac{4\alpha\phi}{3}}F^{2}) \tag{7}$$

Were

$$V(\phi) = \frac{\Lambda}{3(2+\alpha^{2})^{2}}[-12\alpha^{2}(1-\alpha^{2})e^{-\frac{8(\phi-\phi_{0})}{3\alpha}} + 12(4-\alpha^{2})e^{-\frac{4\alpha(\phi-\phi_{0})}{3}} + 72\alpha^{2}e^{-\frac{2(\phi-\phi_{0})(2-\alpha^{2})}{3\alpha}}] \tag{8}$$

The metric for the well-known 5-dimensional dilaton black hole with the cosmological constant is given by:

$$ds^{2} = -f(r)dt^{2} + \frac{1}{f(r)[1-(\frac{r_{-}}{r})^{2}]^{\frac{\alpha^{2}}{\alpha^{2}+2}}}dr^{2} + r^{2}[1-(\frac{r_{-}}{r})^{2}]^{\frac{\alpha^{2}}{\alpha^{2}+2}}d\Omega_{3}^{2} \tag{9}$$

where

$$f(r) = [1-(\frac{r_{+}}{r})^{2}][1-(\frac{r_{-}}{r})^{2}]^{\frac{2-\alpha^{2}}{2+\alpha^{2}}} - \frac{1}{3}\Lambda r^{2}[1-(\frac{r_{-}}{r})^{2}]^{\frac{\alpha^{2}}{2+\alpha^{2}}} \tag{10}$$

$$d\Omega_{3}^{2} = d\theta^{2} + \sin^{2}(\theta)d\phi^{2} + \sin^{2}(\theta)\sin^{2}(\phi)d\varphi^{2} \tag{11}$$

If the solid angle is small, we have black brane,

$$d\Omega_{3}^{2} = \frac{1}{l^{2}}(dx_{1}^{2} + dx_{2}^{2} + dx_{3}^{2}) = \frac{1}{l^{2}}d\vec{x}^{2} \tag{12}$$

Notice r is the radial coordinate that put us from bulk to boundary. In the following we apply dimensionless variable u instead of r, that is $u = (\frac{b}{r})^2$, then

$$ds^2 = \frac{b^2}{u}(1-\frac{a^2}{b^2}u)^{\frac{\alpha^2}{\alpha^2+2}}[-f(u)dt^2 + d\vec{x}^2] + \frac{du^2}{4u^2 f(u)(1-\frac{a^2}{b^2}u)^{\frac{\alpha^2}{\alpha^2+2}}} \tag{13}$$

$$ds^2 = g_{uu}dt^2 + g_{\mu\nu}dx^\mu dx^\nu = g_{MN}dx^M dx^N$$

$$f(u) = -(\frac{u}{b^2}(1-u)\left(1-\frac{a^2}{b^2}u\right)^{\frac{2-2\alpha^2}{2+2\alpha^2}} - \frac{2}{l^2}) \tag{14}$$

Where $\mu, \nu = 0,..,3$, $M, N = 0,..,4$, $M, N = 0,..,4$. $r_+ = b$ and $r_- = a$ are the event horizons. l is the radius spacetime.

3 $\frac{\eta}{s}$ for Dilaton Black Brane Solution

For the calculation of shear viscosity we perturbed the background metric as $g_{\mu\nu} \to g_{\mu\nu} + h_{\mu\nu}$ [5-8]. Considering the abbreviation $h_{\mu\nu} \equiv \phi$, the mode equation is found to be,

$$\frac{1}{\sqrt{-g}}\partial_\mu\left(\sqrt{-g}g^{\mu\nu}\partial_\nu\phi(t,u,\vec{x})\right) = 0 \tag{15}$$

By applying Fourier transformation to $(t,\vec{x})$ coordinates in Eq. (15) and setting the momentum to zero in Green-Kubo formula. Then introducing $\phi(t,u,\vec{x}) = G(u)\phi_0(t,\vec{x})$ where content $\phi_0(t,\vec{x})$ is the source for both graviton in the bulk and the stress tensor on the boundary, we will get,

$$\frac{d^2 G(u)}{du^2} + \frac{1}{2}\left(\frac{H'(u)}{H(u)} + \frac{F'(u)}{F(u)} - \frac{2}{u} + \frac{3B'(u)}{B(u)}\right)\frac{dG(u)}{du} + \frac{\ell^2\omega^2 B(u) - k^2 H(u)}{4\, u\, r_0^2\, F(u)H(u)B(u)}G(u) = 0 \tag{16}$$

With $F'(u) = \frac{dF(u)}{du}$ and $H'(u) = \frac{dH(u)}{du}$.

The long wavelength dynamics of strongly coupled field at boundary can be described in terms of the near horizon data of the black brane solution in the bulk space-time. Therefore, we solve the mode equation close to the horizon,

$$H(u) \approx -(1-u)H'(1) \tag{17}$$

$$F(u) \approx -(1-u)F'(1) \tag{18}$$

$$F(u)H(u) \approx (1-u)^2 F'(1)H'(1) = (1-u)^2(\frac{2\pi\ell^2 T}{r_0})^2 \tag{19}$$

Substituting Eq. (17) - Eq. (19) into the mode equation Eq.(16) gives us,

$$\frac{d^2 G(u)}{du^2} - \frac{1}{1-u}\frac{dG(u)}{du} + \frac{\omega^2}{16\,\pi^2 T^2\,(1-u)^2}G(u) = 0 \tag{20}$$

The above equation has a solution in the form of $G(u) = (1-u)^\beta$. By putting this ansatz into the Eq. (20) we can obtain β,

$$\beta = \pm\frac{I\varpi}{2}, \qquad \varpi = \frac{\omega}{2\pi T} \tag{21}$$

Retarded Green's function on the boundary corresponds to the ingoing mode of near horizon. Due to event horizon properties the outgoing mode doesn't exist. By putting the outgoing solution aside, we will have,

$$G(u) = (1-u)^{-\frac{I\varpi}{2}} \tag{22}$$

Here we consider the following ansatz for the mode equation Eq. (21),

$$G(u) = \tilde{F}(u)^{-\frac{I\varpi}{2}}(\tilde{h}_0(u) + \frac{I\varpi}{2}\tilde{h}_1(u) + O(\varpi^2)) \tag{23}$$

where $\tilde{F}(u) = \sqrt{F(u)H(u)}$ Since we want to normalize $G(u)$ on the boundary, we choose $\tilde{h}_0(u) = 1$.

For determining $\tilde{h}_1(u)$ we plug (23) in (16) and keep to first order of ϖ,

$$\boldsymbol{\tilde{h}_1{}'' + \left(\frac{\tilde{F}'(u)}{\tilde{F}(u)} - \frac{1}{u} + \frac{3B'(u}{B(u)}\right)\tilde{h}_1{}' - \frac{\tilde{F}''}{\tilde{F}} + \frac{\tilde{F}''}{\tilde{F}}(\frac{1}{u} - \frac{3B'(u)}{B(u)}) = 0} \tag{24}$$

It can be easily solved to find,

$$\boldsymbol{\frac{\tilde{F}\tilde{h}_1{}' - \tilde{F}'}{u\, B(u)^{\frac{-3}{2}}} = C_1} \tag{25}$$

$$\boldsymbol{\tilde{h}_1 = log\frac{\tilde{F}}{C_2} + C_1\int_b^u \frac{n\, B(n)^{\frac{-3}{2}}}{\tilde{F}(n)}dn} \tag{26}$$

where C_1 and C_2 are integration constants. For our purposes the explicit form of $\tilde{h}_1$ is not important. It would be enough to find C_1 by demanding $\tilde{h}_1$ to be nonsingular at the horizon. So, we may investigate the near horizon behavior of the integral in (26) as follows,

$$\boldsymbol{\tilde{F} \approx -(1-u)\tilde{F}'(1) = -(1-u)\frac{2\pi l^2 T}{b}} \tag{27}$$

$$\boldsymbol{\tilde{h}_1 \approx log\frac{1-u}{C_2} - \frac{C_1 B(u=1)^{\frac{-3}{2}} b}{2\pi l^2 T} log\,(1-u)} \tag{28}$$

To have non-singular $\tilde{h}_1$ at the horizon, C_1 is chosen to be,

$$\boldsymbol{C_1 = \frac{2\pi l^2 T}{b}B(u=1)^{\frac{3}{2}}} \tag{29}$$

The prescription for calculation of retarded Green's function is presented by Son [5-7]. We calculate retarded Green's function by this prescription as follows:

$$G^R(x-y) = -\sqrt{-g}\,g^{uu}G^*(u)\partial_u G(u)|_{u\to 0} = \frac{I\,\omega\,b^4}{\pi l^5 T}\left(\frac{\widetilde{F}' - \widetilde{F}\widetilde{h}_1{}'}{u\,B(u)^{\frac{-3}{2}}}\right)|_{u\to 0}$$

$$= -\frac{I\,b^4\omega}{\pi l^5 T}C_1 = -\frac{I\,b^3\omega}{l^3}g(u=1)^{\frac{3}{2}} \tag{30}$$

Now we can calculate shear viscosity by using Green-Kubo formula

$$\eta = -\lim_{\omega\to 0}\frac{1}{\omega}ImG^{xx}_{yy}(\omega,\vec{0}) = \frac{b^3}{l^3}g(u=1)^{\frac{3}{2}} \tag{31}$$

The entropy can be found by using Hawking-Bekenstein formula

$$S = \frac{A}{4G} = \frac{b^3\,V_3}{4\,G\,l^3}g(u=1)^{\frac{3}{2}} \tag{32}$$

The entropy density,

$$s = \frac{S}{V_3} = \frac{A}{4G} = \frac{b^3}{4\,G\,l^3}g(u=1)^{\frac{3}{2}} \tag{33}$$

where V_3 is the volume of the constant t and r hyper-surface with radius r_0 and in the last line we used $\frac{1}{16\pi G} = 1$ so $\frac{1}{4\pi} = 4G$. Then the ratio of shear viscosity to entropy density is,

$$\frac{\eta}{s} = \frac{1}{4\pi} \tag{34}$$

4 Results and Discussion

We showed that the lower bound of the $\frac{\eta}{s}$ preserves for Dilaton black brane. This bound is known as KSS conjecture [6] and considered for strongly interacting systems where reliable theoretical estimate of the viscosity is not available. It tells us that the $\frac{\eta}{s}$ has a lower bound, $\frac{\eta}{s} \geq \frac{\hbar}{4\pi k_B}$, for all relativistic quantum field theories at finite temperature without chemical potential and can be interpreted as the Heisenberg uncertainty principle [5]. This conjecture violates for higher derivative gravities like the Gauss-Bonnet gravity [8]. The ratio of shear viscosity per entropy density is proportional to the inverse square coupling of quantum thermal field theory, $\frac{\eta}{s} \sim \frac{1}{\lambda^2}$, where λ is the coupling constant of field theory. In particular, the stronger the coupling, the weaker the shear viscosity per entropy density. In theories with gravity duals, even in the limit of infinite coupling the ratio $\frac{\eta}{s}$ cannot be made smaller than $\frac{1}{4\,\pi}$. Therefore, the dual of Dilaton black brane is the same as Schwarzschild black brane.

5 Conclusions

We showed that KSS bound is saturated for Dilation black brane and the coupling of field theory dual of our model and Schwarzschild black brane is the same.

References

[1] J. M. Maldacena, “The large N limit of superconformal field theories and supergravity,” Adv. Theor. Math. Phys. 2 (1998) 231 [Int. J. Theor. Phys. 38 (1999) 1113]

[2] G. Policastro, D. T. Son, and A. O. Starinets, The shear viscosity of strongly coupled N = 4 supersymmetric yang-mills plasma, Phys. Rev. Lett. 87 (2001) 081601

[3] S. Bhattacharyya, V. E. Hubeny, S. Minwalla, and M. Rangamani, Nonlinear fluid dynamics from gravity, JHEP 0802 (2008) 045

[4] C. J. Gao and S. N. Zhang, Higher dimensional dilaton black holes with cosmological constant," Phys. Lett. B 605 (2005) 185

[5] P. Kovtun, D. T. Son, and A. O. Starinets, Viscosity in strongly interacting quantum field theories from black hole physics, Phys. Rev. Lett. 94 (2005) 111601

[6] A. Buchel and J. T. Liu, “Universality of the shear viscosity in supergravity,” Phys. Rev. Lett. 93 (2004) 090602

[7] P. Kovtun, D. T. Son and A. O. Starinets, “Viscosity in strongly interacting quantum field theories from black hole physics,” Phys. Rev. Lett. 94 (2005) 111601

[8] M. Brigante, H. Liu, R. C. Myers, S. Shenker and S. Yaida, Viscosity Bound Violation in Higher Derivative Gravity," Phys. Rev. D 77 (2008) 126006

Talk link: https://aparat.com/v/cCQwo

Wednesday 9th March 2022

Abstract - Oral

Pole – Skipping in D3/D7 Holographic Model

Mahdi Atashi [1], Kazem Bitaghsir Fadafan[1],
[1] Faculty of Physics, Shahrood University of Technology, P.O. Box 3619995161, Shahrood, Iran.
Email: m.atashi@shahroodut.ac.ir
[1] Faculty of Physics, Shahrood University of Technology, P.O. Box 3619995161, Shahrood, Iran.
Email: bitaghsir@shahroodut.ac.ir

Abstract. We consider SU(N_c) $\mathcal{N} = 4$ SYM theory coupled to N_f flavors $\mathcal{N} = 2$ hypermultplets and study the pole skipping phenomena in the dual gravity background. It is shown that the near horizon analysis of scalar field in this background is different and does not lead to pure imaginary points in the frequency and momentum plane.

Keywords: Pole - skipping, D3/D7 model, Holography

Talk link: https://holography.du.ac.ir/en/files.php?rid=20

Wednesday 9th March 2022

Abstract – Poster

Sultana's generalization of Wyman's scalar field solution and it's Brans-Dicke relative

Ali Banijamali
Babol Noshirvani University of Technology, Iran
Email: a.banijamali@nit.ac.ir

Abstract. Wyman's less known static and spherically symmetric solution of the Einstein-Klein-Gordon equations and its recent generalization for a positive cosmological constant are discussed, showing that they contain central naked singularities. By mapping back to the Jordan frame, we obtain the conformal cousins of these geometries that solve the vacuum Brans-Dicke field equations and are time dependent and spherical.

Keywords: Spherically symmetric solution, Brans-Dicke theory, Conformal transformation

Talk link: https://holography.du.ac.ir/en/files.php?rid=19

Wednesday 9th March 2022

Abstract – Poster

Charged BTZ black hole in AdS3/BCFT2

Fabiano Francisco Santos
Instituto de Física, Universidade Federal do Rio de Janeiro, Brazil.
Email: fabiano.ffs@gmail.com

Abstract. In this paper, we present the charged BTZ black hole in AdS3/BCFT2 correspondence. In this duality, we have systems with boundaries, in particular, boundary known as Conformal Field Theories (BCFTs). In our study, we consider a gravity system with a BTZ black hole coupled with a Maxwell field. We will show as the boundary's theories are modify by the electric charge, which they're gone solved to a holographic description for AdS3/BCFT2 correspondence in our study. Such boundaries are evaluated by numerical procedures and finite small chemical potential where can find a holographic current for BCFT2. Beyond of this result's, we evaluate the analogous of the fluid/gravity correspondence in presence of the electric field.

Keywords: AdS3/CFT2 correspondence, Electric field, Fluid/gravity correspondence

Talk link: https://holography.du.ac.ir/en/files.php?rid=22

Wednesday 9th March 2022

Abstract - Poster

Higher order perturbation corrections on the stability of SBdS black hole

Hoda Farahani
School of Physics, Damghan University, Damghan, Iran
Email: h.farahani@umz.ac.ir

Abstract. In this work, higher-order correction of the entropy is considered and the thermodynamical properties of Schwarzschild–Beltrami–de Sitter black hole is studied. By using the corrected entropy and Hawking temperature, some thermodynamical quantities like Gibbs and Helmholtz free energies and heat capacity are extracted. We find that presence of higher-order corrections, may remove some instabilities of the black hole. Also unstable to stable phase transition is possible in presence of the first- and second-order corrections. This presentation is based on arXiv:1701.08650.

Keywords: Black hole, Thermodynamics, Quantum correction

Talk link: https://www.aparat.com/v/17w4D

Wednesday 9th March 2022

Abstract – Oral

Quantum Corrections to the Shadow of Schwarzschild Black Hole Surrounded by Holographic Quintessence

Sara Saghafi[1], Kourosh Nozari[2]
[1]Department of Theoretical Physics, University of Mazandaran, Babolsar. Iran
Email: s.saghafi@umz.ac.ir
[2]Department of Theoretical Physics, University of Mazandaran, Babolsar. Iran
Email: knozari@umz.ac.ir

Abstract. We study the shadow behavior of a quantum-corrected, regular Schwarzschild black hole surrounded by the holographic quintessence. We investigate how the shadow of a black hole is influenced by quantum effects together with holographic quintessence. We use the Hamilton-Jacobi approach and also, the Carter method to formulate the geodesic equations of the black hole. We find that the shadow size of a black hole is indeed determined by background quantum effects and dark energy ingredient of the Universe, in addition to the mass of a non-rotating black hole.

Keywords: Holographic quintessence, Shadow, Regular black holes.

Talk link: https://www.aparat.com/v/CFRXx

Thursday 10th March 2022

Abstract – Oral

Axial-vector form factor of nucleons at finite temperature from the AdS/QCD soft-wall model

Shahin. A. Mamedov [1], Narmin Nasibova [2],
[1] Institute for Physical Problems, Baku State University, Baku, Azerbaijan,
[1] Theoretical Physics Department, Physics Faculty, Baku State University, Baku, Azerbaijan,
[1] Instutute of Physics, Azerbaijan National Academy of Sciences, Baku, Azerbaijan.
Email: sh.mamedov62@gmail.com
[2] Instutute of Physics, Azerbaijan National Academy of Sciences, Baku, Azerbaijan.
Email: n.nesibli88@gmail.com

Abstract. The axial-vector form factor of the nucleons is considered at finite temperature using the holographic soft-wall model having the thermal dilaton field. We use bulk interaction action known from the zero-temperature case and apply in it the profile functions of fields, which are thermalized by both the AdS-Schwarzschild metric and by the interaction with the thermal dilaton. Dependencies from the squared momentum transfer and the temperature are plotted for the ground and excited states of the nucleons.

Keywords: AdS/QCD, Holography, Soft-wall model, Axial-vector, Form factor.

Talk link: https://aparat.com/v/RDKBT

Thursday 10th March 2022

Abstract – Oral

A thermodynamic geometry approach for a black hole in modified gravity

Saheb Soroushfar
[1]Yasouj University, Iran
Email: saheb.soroushfar@gmail.com

Abstract. In this paper, we consider a black hole in modified gravity and study the thermodynamic geometric approach for this black hole. Thermodynamic quantities like the heat capacity, entropy and the temperature are analyzed. The stability of the system is emphasized from the heat capacity analyze. Moreover, following thermodynamic geometry formalism, thermodynamic geometry of this black hole in modified gravity is also investigated.

Keywords: Black hole, Heat capacity, Thermodynamic geometry, Modified gravity.

Talk link: https://holography.du.ac.ir/en/files.php?rid=9

Thursday 10th March 2022

Abstract - Oral

Thermodynamics of the Van der Waals cosmic fluid

Mahasweta Biswas[1], Sayani Maity[2], Ujjal Debnath[3]
[1] Instutute of Physics, Azerbaijan National Academy of Sciences, Baku, Azerbaijan.
Email: mahasweta.bsc11@gmail.com
[2] Indian Institute of Engineering Science and Technology, Shibpur
Email: sayani.maity88@gmail.com
[3] Indian Institute of Engineering Science and Technology, Shibpur,
Email: ujjaldebnath@gmail.com

Abstract. This paper is devoted to investigate the thermodynamic stability of a generic cosmological fluid known as Van der Waals fluid in the context of flat FRW universe. It is treated as a perfect fluid that obeys the equation of state $P = \frac{\gamma\rho}{1-\beta\rho} - \alpha\rho^2, \ \ 0 \leq \gamma < 1$, where ρ stands for energy density and P stands for pressure of the fluid. In this regard, we discuss the behavior of physical parameters to analyze the evolution of the universe. We investigate whether the cosmological scenario fulfills the third law of thermodynamics using specific heat formalism. Next, we discuss the thermal equation of state and by means of adiabatic, specific heat and isothermal conditions from classical thermodynamics we examine the thermal stability.

Keywords: Dark Energy, Van der Waals cosmic fluid.

Talk link: https://aparat.com/v/AgMQB

Thursday 10th March 2022

Abstract - Oral

Chaos in a QQ-bar system at finite temperature and baryon density

Nicola Losacco[1], Pietro Colangelo[2], Fulvia De Fazio[3]
[1] Università degli studi di Bari, Italy
Email: nicola.losacco@ba.infn.it
[2] National Institute for Nuclear Physics, Italy
Email: pietro.colangelo@ba.infn.it
[3] National Institute for Nuclear Physics, Italy
Email: Fulvia.defazio@ba.infn.it

Abstract. Onset of chaos for the holographic dual of a QQ-bar system at finite temperature and baryon density is studied. We consider a string in the AdS Reissner–Nordstrom background near the black-hole horizon and investigate small time-dependent perturbations of the static configurations. The proximity to the horizon induces chaos, which is softened increasing the chemical potential. A background geometry including the effect of a dilaton is also examined. The Maldacena, Shenker, and Stanford bound on the Lyapunov exponents characterizing the perturbations is satisfied for finite baryon chemical potential and when the dilaton is included in the metric.

Keywords: AdS/CFT Correspondence, MSS Bound on Chaos.

Talk link: https://www.aparat.com/v/i8BmE

Thursday 10th March 2022

Full paper – Poster

A fork grating with controllable vortex diffraction order

Parisa Soleimani[1], Habib Khoshsima[2], Mohammad Yeganeh[3]
[1] Research Institute for Applied Physics and Astronomy, University of Tabriz, Tabriz, Iran
Email: p_soleimani@tabrizu.ac.ir
[2] Research Institute for Applied Physics and Astronomy, University of Tabriz, Tabriz, Iran
Email: khoshsima@tabrizu.ac.ir
[3] Department of Physics, Institute for Advanced Studies in Basic Sciences (IASBS), Zanjan, Iran
Email: moyeganeh@iasbs.ac.ir

Abstract. It is well known that optical vortices have great potential in optical communications, quantum computations, micro-manipulation, and many other applications. Controlling the diffraction order of the beam vortices is still a challenge. Our system consists of a planar dye-doped liquid crystal (DDLC) cell that has a fork-grating lithography mask printed on it. Changing the diffraction order of fork grating diffractions can be accomplished by applying an electric field to the cell. Therefore, a fork-shaped phase profile can be obtained characterized by the alternation of ordinary and extraordinary refractive indices. The devices allow for the control of vortex diffraction order, as well as excellent polarization independence and high efficiency.

Keywords: Diffraction order, Fork grating, Optical vortex beam, Refractive index

Introduction

In the past two decades, optical vortices have attracted considerable attention and have been extensively studied. An optical vortex is a beam of light characterized by a helical phase front. Thus, the wavefront is twisted like a corkscrew around its propagation axis [1]. There are a number of phase windings in one wavelength known as the topological charge, which represents the phase rotation velocity around the axis. Phase windings are (or topological charge, m) a key property of these vortices. In order for an optical vortex to maintain continuity, m must be an integer [2,3]. Thus, orbital angular momentum (OAM) is quantized. Phase singularity at the axis causes no intensity, which results in a donut-shaped distribution of intensity. Depending on the topological charge, the shape of the ring is determined. Topological charge and its corresponding OAM provide a new level of freedom in characterizing the properties of a light beam, thereby opening up new applications and even uncharted terrain.[4] According to theory, optical vortices contain an infinite number of states as a result of their unlimited topological charge [3].

In addition to characterizing the light properties by determining their orbital angular momentum (OAM), it opens the doors to widespread applications in informatics, micromanipulation, and astronomy [5]. In quantum computing, OAM multiplexing can be used to encode and store information based on the multiple states of light [1], which are created by the vortices in light. Optical vortex coronagraphs increase the contrast of astronomical observations by blocking the strong background light, which is useful for searching for extrasolar planets. Optical vortices have a wide range of applications in fields such as informatics, micro-manipulation, and astronomy [2]. In order to generate optical vortices, several techniques have been developed. A cylindrical lens mode converter was used in the initial research to realize Laguerre-Gaussian mode vortices [6]. Consequently, spiral phase plates have been used to produce optical vortex by directly rephasing plane waves [1,7]. The electro-optical (EO) properties of liquid crystals (LCs) have led to the development of tunable vortex generators [8,9]. LC spiral phase plates or fork gratings for controlling diffraction order of optical vortices are typically made with liquid crystal cells [10].

In this work, a controllable diffraction order optical vortex generator is demonstrated via a dye-doped E7 liquid crystal cell driven by an electric field. Based on the printed fork grating lithography mask on DDLC, it can control the diffracted order of vortex beams. Furthermore, it switches the diffracted order of the fork grating vortex beams independent of incident polarization.

Generation of optical vortex

In order to generate optical vortices, several techniques have been developed. However, it has a bulky and complex optical setup, which makes it difficult to generate beam vortices with large m numbers. One of the ways for generating an optical vortex beam is fork grating. Fork gratings are diffraction gratings with dislocations in the center, which offer an efficient method of generating beam vortices [8,9,10]. A fork grating can convert a Gaussian beam into a series of helical phases, each with its own twist direction. Currently, this is a very convenient way to generate beam vortices. The phase function of an optical vortex can be described by $\Psi 1 = \exp(im\theta)$ (Figure 1 a), where θ is the azimuthal angle of a cylindrical coordinate system (r, θ, z) around the z-axis, which indicates the beam propagation direction, m is the topological charge and can be positive or negative, depending on the direction of the twist (positive for counterclockwise rotation and negative for clockwise rotation) [2].

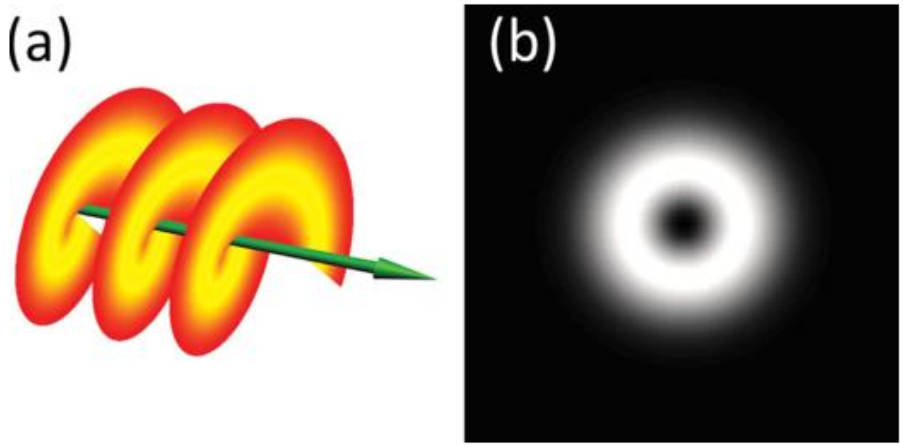

Figure 1: a) The helical wave fronts of a vortex beam with m=1 calculated according to $\psi_1 = exp(im\theta)$ b) normalized intensity distribution when the beam is viewed against the propagation axis [2].

The interference between plane wave $\psi_2(x) = exp(ikx)$ (where k is the spatial frequency, which indicates the wavenumber) and an object wave $\psi_1 = exp(im\theta)$. The interference pattern could be described by the function [1-3]:

$$H = |\psi_1 + \psi_2| = |exp(im\theta) + exp(ikx)|^2 = 2[1 + cos(kx - m\theta)]$$

where $\theta = tan^{-1}(^y/_x)$ is the polar coordinate. Figure 2 shows the fork grating simulation for m=1.

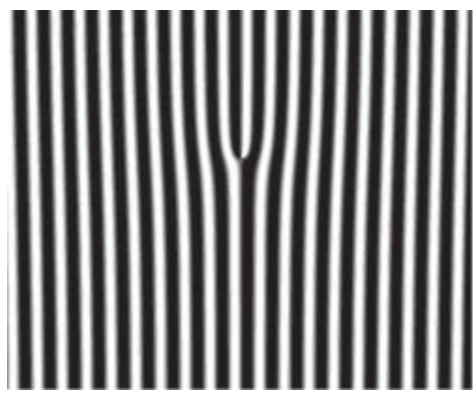

Figure 2: simulated holograms according to equation (1) for m=1 [1].

Experimental

For generating and controlling diffraction order of vortex beam, was used the nematic homogeneous liquid crystal E7 dopped by methyl red (MR) in $20\mu m$ cell, and a fork grating lithography mask. It was written by 532nm laser which is beam lighting a sample about normal incidence for writing the fork-grating might on DDLC, it was shown in FIG. 2. By applying electric field on cell the diffraction of the He-Ne probe beam showed that the grating originates from a reorientation of the director in the plane of incidence. This reorientation was first attributed to a photorefractive-like effect. Experimental schematic of setup for the generation vortex beam was shown in (Figure. 3).

L_2

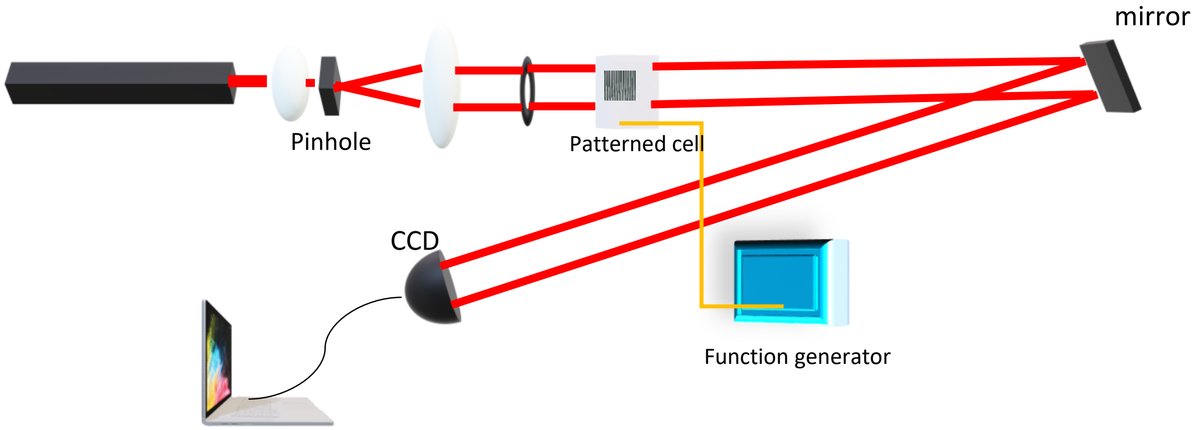

Figure 3: schematic diagram of generation vortex beam and controlling diffraction order

Figure 3 shows the experimental setup for characterizing the phase grating. A He-Ne laser ($\lambda = 632nm$) was used as probing beam. The incidence beam is collimated and unpolarized which illuminated cell. After the cell is put a mirror for reflecting light onto CCD. In addition, the intensity of each order was detected by a CCD in the far-field located at a distance of ~194cm. Figure 4 shows the recorded diffractions orders of fork grating which is printed onto DDLC by applying voltage it can be shown the diffraction order of the generation vortex beam can be changed.

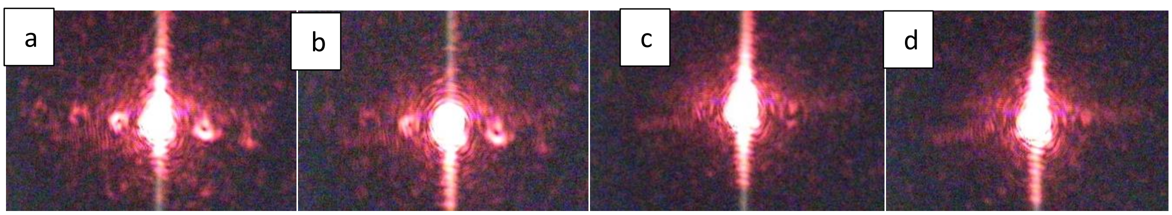

Figure 4:diffraction order of DDLC by applying electric field a)v=1.72v b) v=2.59v c)14.1v d)22.1v

Conclusion

In the described system a fork-grating lithography mask is printed on DDLC planar cell. Changing the diffraction order of fork grating diffractions can be accomplished by applying an electric field to the cell which is shown in Figure 4. When the applied voltage is increased the diffraction order of generated vortex beam is being to disappears. Therefore, it can be obtained the alternation of ordinary and extraordinary refractive indices varying by changing the applied voltage. The devices allow for the control of vortex diffraction order, as well as excellent polarization independence.

References

[1] Alison M. Yao and Miles J. Padgett, "Orbital angular momentum: origins, behavior and applications," Adv. Opt. Photon. 3, 161-204 (2011)

[2] Wei, B.-y., Hu, W., Ming, Y., Xu, F., Rubin, S., Wang, J.-g., Chigrinov, V., and Lu, Y.-q, "Generating Switchable and Reconfigurable Optical Vortices via Photopatterning of Liquid Crystals," Adv. Mater., 26: 1590-1595(2014).

[3] Deng, Duo, Zhao, Hua, Ni, Jincheng, Li, Yan and Qiu, Cheng-Wei. "A phase-to-intensity strategy of angular velocity measurement based on photonic orbital angular momentum" Nanophotonics, vol. , no. , 2021, pp. 000010151520210461.

[4] Lee, D., Lee, H., Migara, L. K., Kwak, K., Panov, V. P., Song, J.-K., Widely Tunable Optical Vortex Array Generator Based on Grid Patterned Liquid Crystal Cell. *Adv. Optical Mater* (2021).

[5] Luyi Wang, Jiantao Ma, Min Xiao, Yong Zhang," Application of optical orbital angular momentum to rotation measurements," Results in Optics, Volume 5,(2021).

[6] P. Pradhan, M. Sharma, and B. Ung, "Generation of Perfect Cylindrical Vector Beams With Complete Control Over the Ring Width and Ring Diameter," in *IEEE Photonics Journal*, vol. 10, no. 1, pp. 1-10 (2018).

[7] Rotschild, Carmel, et al. "Adjustable spiral phase plate." *Applied Optics* 43.12 (2004).

[8] Zheng, Shuiqin, et al. "Liquid crystal-based order electrically controlled q-plate system." *Optics Express* 27.11 (2019).

[9] Andrienko, Denis. "Introduction to liquid crystals." *Journal of Molecular Liquids* 267 (2018).

[10] Marco, David, et al. "Using birefringence colors to evaluate a tunable liquid-crystal q-plate." *JOSA. B* 36.5 (2019).

Talk link: https://holography.du.ac.ir/en/files.php?rid=26

Wednesday 9th March 2022

Full paper – Poster

Study of the Penrose process at WGC condition for the charge rotating BTZ black holes

Elaheh Naghd Mezerji[1], Jafar Sadeghi[2], Tahereh Azizi[3]
[1]Department of Physics, Faculty of Basic Sciences, University of Mazandaran, Babolsar, Iran
Email: e.n.mezerji@stu.umz.ac.ir
[2]Department of Physics, Faculty of Basic Sciences, University of Mazandaran, Babolsar, Iran
Email: pouriya@ipm.ir
[3]Department of Physics, Faculty of Basic Sciences, University of Mazandaran, Babolsar, Iran
Email: t.azizi@umz.ac.ir

Abstract. In this paper, we study the collision of spinning particles near a charged rotating BTZ black hole with WGC condition, and we obtain the extracted energy of the black hole by the Penrose process. We assume two particles fall from infinity and collide near a black hole. During this collision, one particle falls into the black hole, and the other escapes to infinity. We examine and calculate the maximum efficiency parameter (η). We mention that by exerting the weak gravity conjecture, we have $\eta max \simeq 1250$. On the other hand, the particles created in the collision have a specific range of spin, which can lead to the formation of unknown particles. This result can enhance our understanding of how black holes work, how they die, and better study physical, astronomical black holes. A thorough understanding of black holes helps us understand how a holographic system works.

Keywords: AdS/CFT Correspondence, MSS Bound on Chaos.

Talk link: https://holography.du.ac.ir/en/files.php?rid=14

Wednesday 9th March 2022

1 Introduction

Studying spinning and non-spinning particles collisions near the background of black holes has a long history. The energy extracted from the black hole is much more efficient than nuclear energy. It can be extracted from certain black holes (rotating). The possibility of a particles collision near a black hole was first investigated by Piran and others in 1975 [1]. In the continuation of this path, discovered a new particle collision mechanism by Banados, Silk, and West (BSW), in 2009 [2]. In recent years, different black holes have studied various aspects of the BSW mechanism. Many results have been investigated, such as Kerr naked singularity and rotating black holes and their universal properties [3]. The Penrose process has a wide range of applications. We assume the particles that fall into the ergo region of the black holes are broken into two particles. The broken particle sinks into the black hole with negative energy, and another escapes to infinity with positive energy. The resulting energy extraction from rotating black holes is called the Penrose process. This method is expected to provide a more efficient mechanism in astrophysical conditions. Unknown particles can form at high energies, indicating new physics [4]. In this article, we peruse BTZ black Holes. A specific stationary black hole solution was first investigated for three-dimensional space-time with a negative cosmological constant by Banados-Teitelboim-Zanelli (BTZ) [5]. This beautiful model helps to gain a deep understanding of the BTZ background. Many problems are simpler and more analytical in the BTZ space-time than in Kerr [6]. In the study of particle collision, many authors usually focus on particle geodetic path, so the motion equations of spinning particles around a space-time background are described by Mathisson-Papapetrou-Dixon (MPD) equations [7]. Here, we take advantage of the collisions associated with the Kerr space and investigate the particle collision on the CR BTZ black hole. Also, the weak gravity conjecture (WGC) plays a significant role in this paper. Most recently, WGC has been studied in various fields, including aspects of this conjecture, such as swampland

and landscape. In those cases, we can say the theories set inconsistent and consistent with quantum gravity are swampland and landscape, respectively. Generally, for different applications of WGC, one can see Refe.s [8–11]. As we know, black holes have extremal conditions ($Q = M$) in the WGC. This condition is slightly different in rotating black holes. In general, the weak gravity conjecture can have new practical aspects. This article examines the energy obtained from the collision of two spinning mass particles from the BSW method at WGC conditions. The above discussions motivate us to organize the corresponding paper as a following. Section 2 thoroughly examines the collision of spinning particles near the CR BTZ black hole to BSW methods. In section 3, we study the WGC condition and two essential constraints that orbits create on particles. Section 4 examines the process performed in section 2 with the WGC method. Moreover, in the final section, we examine the results obtained.

2 The motion equations of spinning particles

One of the extraordinary phenomena to investigate extracted energy is colliding two spinning mass particles near a charged rotating black hole. For this reason, first, we consider the metric of CR BTZ black hole, which is given by

$$ds^2 = -(-M + \frac{r^2}{l^2} + \frac{j^2}{4r^2} - \frac{\pi Q^2 \log(r)}{2})dt^2 + \frac{dr^2}{(-M + \frac{r^2}{l^2} + \frac{j^2}{4r^2} - \frac{\pi Q^2 \log(r)}{2})} + r^2(d\phi + \frac{j}{2r^2}dt)^2 \quad (1)$$

Here M, Q and j are mass, charge and angular momentum of black hole respectively and $l^2 = (-\frac{3}{\Lambda})$, $8G = c = 1$. According to the space-time background, the equations of motion can be calculated with MPD equations.

$$\frac{DP^a}{D\tau} = -\frac{1}{2}R^a_{bcd}v^b S^{cd}, \qquad \frac{DS^{ab}}{D\tau} = P^a v^b - P^b v^a \tag{2}$$

Here $v^a = (\frac{\partial}{\partial r})^a$, $\frac{D}{D\tau}$, P^a and S^{ab} are tangent vector, covariant derivative, 4-momentum and the spin tensor, respectively. We use $S^{ab}P_b = 0$ and $P^a v_a = -m$ to get logical relations between P^a and v^a. By combining these equations, one can obtain $mv^a - P^a = \frac{S^{ab}R_{bcde}P^c S^{de}}{2(m^2+\frac{1}{4}R_{bcde}S^{bc}S^{de})}$. Generally, we know that 4-momentum is not parallel to 4-speed of spin particles in $4-$dimensions. Of course, our space-time will be $(2+1)-$dimensions. For two killing vectors in CR BTZ space-time $\zeta^a = (\frac{\partial}{\partial t})^a$ and $\phi^a = (\frac{\partial}{\partial \phi})^a$. So, the corresponding conserved quantity concerning ζ^a will be as, $Q_\zeta = P^a\zeta_a - \frac{1}{2}S^{ab}\nabla_b\zeta_a$. By using the above equation, we can calculate the two conserved equations, which are energy per unit mass E_m and angular momentum per unit mass J_m. we can obtain

$$\begin{aligned}
E_m &= -u^a\zeta_a + \frac{1}{2m}S^{ab}\nabla_b\zeta_a = \sqrt{f(r)}u_0 + (\frac{j}{2r} - \frac{\pi s Q^2}{4r} + \frac{sr}{l^2})u_2,\\
J_m &= u^a\phi_a - \frac{1}{2m}S^{ab}\nabla_b\phi_a = s\sqrt{f(r)}u_0 + (-\frac{2r^3}{j} - \frac{j^2 s}{4r^3} - \frac{\pi s Q^2}{4r} + \frac{rs}{l^2} - \frac{2r^3 s}{j-2r^2})u_2.
\end{aligned} \tag{3}$$

The above equations help us to obtain the dynamic velocity u by using $(u_0)^2 - (u_1)^2 - (u_2)^2 = m^2$.

$$\begin{aligned}
u_0 &= \frac{E_m(-4r - \frac{2js}{r}) + J_m(\frac{2j}{r} - \frac{\pi s Q^2}{r} + \frac{4rs}{l^2})}{(-4r - \frac{\pi s^2 Q^2}{r} + \frac{4rs^2}{l^2})\sqrt{f(r)}},\\
u_2 &= \frac{J_m - E_m s}{r + (\frac{\pi Q^2}{4r} - \frac{r}{l^2})s^2},\\
u_1 &= \rho\sqrt{-m^2 - \frac{16(J_m - E_m s)^2}{(-4r - \frac{\pi s^2 Q^2}{r} + \frac{4s^2 r}{l^2})^2} + \frac{(E_m(-4r - \frac{2js}{r}) + J_m(\frac{2j}{r} - \frac{\pi s Q^2}{r} + \frac{4rs}{l^2}))^2}{(-4r - \frac{\pi s^2 Q^2}{r} + \frac{4rs^2}{l^2})^2 f(r)}}.
\end{aligned} \tag{4}$$

By using the above equations with appropriate replacements, one can obtain v_0, v_1 and v_2 as,

$$v_0 = (-4r - \frac{\pi s^2 Q^2}{r} + \frac{4rs^2}{l^2})u_0, \qquad v_1 = (-4r - \frac{\pi s^2 Q^2}{r} + \frac{4rs^2}{l^2})u_1, \qquad v_2 = (-4r + \frac{\pi s^2 Q^2}{r} + \frac{4rs^2}{l^2})u_2 \tag{5}$$

The motion equation of spinning particles in the CR BTZ space-time can be calculated according to the above equations, and where $P_0 = P^t(r), P_1 = P^r(r)$, $P_2 = P^\phi(r)$ and $\rho = \pm$. We note that the sign $+$ and $-$ indicate the particle direction is outward and inward, respectively.

$$\begin{aligned}
\frac{P_0}{m} =& (\frac{E_m(-4r - \frac{2js}{r}) + J_m(\frac{2j}{r} - \frac{\pi s Q^2}{r} + \frac{4rs}{l^2})}{\sqrt{f(r)}}),\\
\frac{P_1}{m} =& \rho[\frac{(J_m(\frac{2j}{r} - \frac{\pi s Q^2}{r} + \frac{4rs}{l^2}) - E_m(4r + \frac{2js}{r}))^2}{f(r)} - (4r + \frac{\pi s^2 Q^2}{r} - \frac{4rs^2}{l^2})^2 m^2 - 16(J_m - E_m s)^2]^{\frac{1}{2}},\\
\frac{P_2}{m} =& 4(-4r + \frac{\pi s^2 Q^2}{r} + \frac{4rs^2}{l^2})(\frac{J_m - E_m s}{4r + \frac{\pi s^2 Q^2}{r} - \frac{4rs^2}{l^2}}).
\end{aligned} \tag{6}$$

3 The constraints

Generally, one can say that the extreme black holes must be unstable in any corrected theory as a quantum gravity (except in cases we have symmetry). As we know, the extreme condition $M = Q$ causes us to consider a state like $\frac{q}{m} \geq 1$. The essential point here is that we will have a completely different extreme condition for charged rotating black holes, so in this case, we have,

$$M^2 = Q^2 + \frac{J^2}{M^2}. \tag{7}$$

We continue our calculations by placing condition WGC in the motion equations of the previous section. Particles collide in r with $r \geq r_H$ condition, where r_H is the event horizon radius of a black hole. They reach the collision point in the ergo region of a black hole with a certain angular momentum and energy. We represent the particular value with the impact parameter $b = \frac{J}{E}$. This point is located

for critical particles b_c on the event horizon r_H. In order to get such a point, the collision point must be before the horizon. Therefore, our first constraint is obtained with $P_1 \geq 0$ and the WGC condition,

$$b = \frac{J_m}{E_m} \geq \frac{4r^2 + 2js}{2j - \pi Q^2 s + 4s(\frac{r}{l})^2}, \tag{8}$$

We can obtain $b_c = \frac{2}{j}$ by the $f(r_h) = f'(r_h) = 0$ conditions. b_c is the critical value, and particles can not reach the horizon under conditions, $b > b_c$. Also, non-critical particles have $b = \frac{2}{j}(1+\gamma)$. Spinning particles must meet the time-like condition to avoid superluminal motions and causality problems. As a result, the second condition is $v^\mu v_\mu < 0$. We obtain,

$$E > \frac{(j^2 s^2 - 4)^2}{16s(js - 2)}. \tag{9}$$

Moreover, we can specify the range of spins as $s_{min} < s < s_{max}$ by placing $E = 1$. In other words, the time-like condition limits the energy and spin of particles. The values obtained are equal to $s = (-2.17, -0.31, 1, 1.48)$. In fig 1, we plot the energy in terms of spin by equation (9). Energy E has only an increasing trend in the range of $-1 < s < 0$.

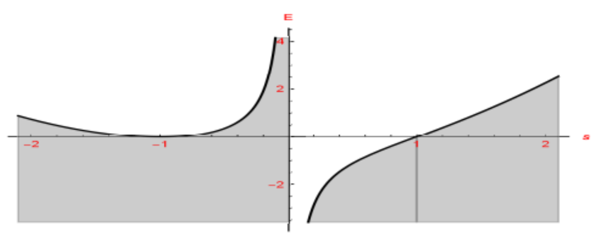

Figure 1: The allowable area indicates the particles' energy E and spins s to reach the event horizon, and particles with the highest energy spin of $-0.6 < s < 0$.

4 The Collision of two massive particles

Now we will investigate the collision of two spinning particles near a charged rotating black hole. The two collide before reaching the horizon. One of the particles falls into the black hole, and the other escapes to infinity. We expect to have maximum energy efficiency. Particles have the following angular momentum: The first critical particle has $J_1 = \frac{2E_1}{j}$, the second non-critical particle has $J_2 = \frac{2E_2}{j}(1+\gamma)$, and The third near-critical particle has $J_3 = \frac{2E_3}{j}(1+\alpha\epsilon+\beta\epsilon^2+..)$. The last particle has an angular momentum based on the other three particles. We use the laws of energy $E_1+E_2 = E_3+E_4$ conservation and angular momentum $J_1+J_2 = J_3+J_4$, and obtain the fourth particle's angular momentum $J_4 = \frac{2}{j}(E_1+E_2(1+\gamma)-E_3(1+\alpha\epsilon+\beta\epsilon^2))$. Also, the spins conditions and direction are equal $s_2 = s_4$, $s_1 = s_3$, $\rho_2 = \rho_4$. These conditions have a good effect on the super-Penrose

process. We assume the mass of particles to be equal $m_1 = m_2 = m_3 = m_4$. Given all these conditions, we calculate the value of P_1 for each particle, and by placing it in equation $P_1^{(1)} + P_2^{(1)} = P_3^{(1)} + P_4^{(1)}$, we can calculate the energy of third particle E_3 based on the first two particles.

$$
\begin{aligned}
E_3 =& \frac{2E_2(\varpi\gamma(1+s_2)^2-1-\varpi+s_2)}{2\varpi^2(2+2s_1+s_1^2+2s_2+s_2^2)}\times \\
& (\pm 2)\sqrt{E_2^2(1+\varpi-s_2-\varpi\gamma(1+s_2)^2)^2 - X\varpi^2(2+2s_1+s_1^2+2s_2+2s_2)}. \\
X =& (\gamma^2E_2^2(1+s_2)^2 - E_2^2(2+\gamma-2s_2) - (2E_1E_2(s_2-1) - E_2^2(2+\gamma-2s_2)+\gamma^2E_2^2(1+s_2)^2)) \\
& + 32\rho_1\rho_2(-2E_2^2(s_1-1)^2(E_1^2+(1+s_1)^2)(s_2-1) + \gamma E_2^2(s_1-1)^2(E_1^2+(1+s_1)^2) - \gamma^2E_2^2 \\
& (s_1-1)^2(E_1^2+(1+s_1)^2)(1+s_2)^2)^{\frac{1}{2}}.
\end{aligned} \tag{10}
$$

We have $\varpi = (\alpha\epsilon+\beta\epsilon^2+...)$ and the following equation obtains the corresponding energy efficiency, $\eta = \frac{E_3}{E_2+E_1}$. Two particles are coming from infinity, so we consider $E_1 \geq 1$ and $E_2 \geq 1$. In order to have the best efficiency, we assume that for the first particle, $\rho_1 = +1$, $E_1 \simeq 1$ and the second particle, $\rho_2 (= \rho_4) = -1$, $E_2 \simeq 1$. So, one can obtain The third particle energy as,

$$
E_3 = \frac{-32(s_1-1)\sqrt{-(2+s_1(2+s_1))}}{2\varpi(s_2+1)}. \tag{11}
$$

Now we need to calculate a γ variable for the second particle. We consider it non-critical $b = \frac{2}{j}(1+\gamma)$ and $E_2 \simeq 1$. By replacing the above-obtained result with the time-like conditions, one can obtain $\gamma = (\frac{s_2+1}{s_2})l^2$. In order to acquire E_3 as a straightforward form, we first take s_2 from equation γ and put it into (11). According to Fig (1), we know that energy has an increasing trend in the range of $-1 < s < 0$. So, we have $s_3 = s_1 = -0.3$ and $\varpi = (\alpha\epsilon+\beta\epsilon^2)$. We can plot E_3 in terms of s_2 and ϖ, fig (2a). This fig shows the highest energy in the lower ϖ, i.e., the third particle has the most energy

E_3, while the second particle s_2 is in a near-critical state. Moreover, when we have the maximum energy, the spin s_2 takes on two values, $0.6 \leq s_2 \leq 0$ and , equal to $0.02 \leq \varpi \leq 0.1$. In the last step, we plot the third particle energy E_3 according to the primary particles spin s_2 and s_1 (Fig (2b)). The third particle has the most energy when the primary particles have spin ranges of $-0.6 \leq s_1 \leq 0$ and $-0.78 \leq s_2 \leq -0.5$. These amounts of energy are for when the primary particles have an energy of $(E/m)_1 \simeq (E/m)_2 \simeq 1$, which means that black holes can extract much energy in the final moments and extremality. So the values obtained above lead us to have the following equation,

$$
\eta = \frac{(E/m)_3}{(E/m)_1+(E/m)_2} \simeq \frac{2500}{2} \simeq 1250. \tag{12}
$$

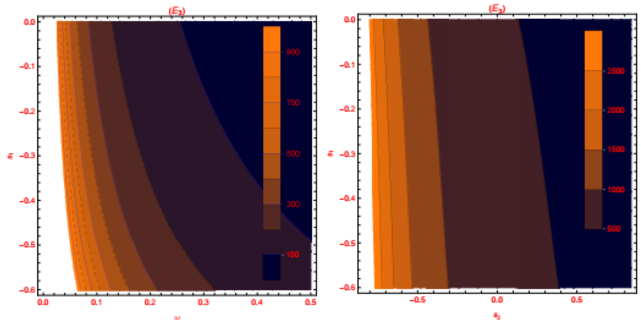

(a) (b)

Figure 2: In (a), we plot the E_3 in terms of ϖ and s_2 whith $\rho_3 = -1$ and $s_1 = s_3 = 0$. In (b), the E_3 in terms of s_1 and s_2, by increasing s_1, the corresponding energy increases.

5 Conclusions

This paper studied the Penrose process for the spinning particles near charged rotating BTZ black holes. In this method, two particles come from infinity and collide near a black hole. One particle falls into a black hole concerning energy and angular momentum, and the other escapes to infinity. We also calculated the maximum efficiency parameter for the third particle and showed that this value equals $\eta \simeq 1250$. These calculations can help us track astrophysics black holes. It will also enhance our understanding of black holes, how they work, and how they die. Black holes can act as a holographic system. How they function and die can lead to exciting studies in their holographic structures, such as thermodynamics and hydrodynamics. We will follow these reviews in future work.

References

[1] T. Piran, J. Shaham, and J. Katz, J. 196, L107 (1975).

[2] M. Banados, J. Silk and S. M. West, Phys. Rev. Lett. 103, 111102 (2009).

[3] M. Patil and P.S. Joshi, Classical Quantum Gravity 28, 235012 (2011).

[4] K. i. Maeda, K. Okabayashi, and H. Okawa, Phys. Rev. D 98, 064027 (2018).

[5] M. Ba˜nados, C. Teitelboim, and J. Zanelli, Phys. Rev. Lett. 69, 1849 (1992).

[6] Kota Ogasawara, and Naoki Tsukamoto, Phys. Rev. 99, 024016 (2019).

[7] P.I. Jefremov, O. Y. Tsupko, and G. S. Bisnovatyi-Kogan, Phys. Rev. D 91, 124030 (2015).

[8] C. Vafa, arxiv:0509212v2 [hep-th] (2005).

[9] J. Sadeghi, S. Noori Gashti and E.Naghd Mezerji.Phys. Dark Univ 30,100626, (2020).

[10] J Sadeghi, EN Mezerji, SN Gashti, Modern Physics Letters A, (2021).

[11] E. Naghd Mezerji, J. Sadeghi, arXiv:2202.12253 [hep-th] (2022).

Full paper (Persian) - Poster

Static Spherical Solution of the Einstein Equations Sourced by a Perfect Fluid

Behnaz Fazlpour
Islamic Azad University, Babol Branch, Iran
Email: b.fazlpour@umz.ac.ir

Abstract. Physical properties of a new classes of solutions of the Einstein equations sourced by a perfect fluid with equation of state P =-(/rho)/5 have been discussed. These geometries depend on up to three parameters and are static and spherically symmetric. They describe compact spaces with naked central singularities and not a black hole or a wormhole throat.

Keywords: Solutions of the Einstein equations, Spherically symmetric, Black hole, Perfect fluid

Full text in Persian is available on https://holography.du.ac.ir/en/files.php?rid=15

Talk link: https://holography.du.ac.ir/en/files.php?rid=18

Wednesday 9th March 2022